International Institute for
Applied Systems Analysis
IIASA www.iiasa.ac.at

The Influence of the Free Troposphere on Boundary Layer Ozone Mixing Ratios over Europe

Wojcik, G.

IIASA Working Paper

WP-95-100

December 1995

Working Paper

The influence of the free troposphere on boundary layer ozone mixing ratios over Europe

Gary Wojcik

WP-95-100
December 1995

IIASA

International Institute for Applied Systems Analysis ☐ A-2361 Laxenburg Austria

Telephone: +43 2236 807 ☐ Telefax: +43 2236 71313

The influence of the free troposphere on boundary layer ozone mixing ratios over Europe

Gary Wojcik

WP-95-100

December 1995

International Institute for Applied Systems Analysis ☐ A-2361 Laxenburg Austria

Telephone: +43 2236 807 ☐ Telefax: +43 2236 71313

Preface

In an effort to determine cost-effective emission control strategies to reduce surface ozone concentrations in Europe, an integrated assessment model for boundary layer ozone is being developed at IIASA. In its current version, the ozone formation and transport module of this integrated assessment model predicts ozone mixing ratios based on annual emissions of nitrogen oxides and volatile organic compounds, both of which play major roles in the ozone problem. One source of ozone that is not currently included as an explicit predictor within this model, however, is the transport of ozone and its precursors from the free troposphere to the boundary layer. The purpose of this paper, then, is to study the influence of the free troposphere on boundary layer ozone mixing ratios and to determine whether or not this free tropospheric influence is significant enough to be included in the model.

Acknowledgments

Many people aided me in completing this work and I extend my greatest appreciation to them. First, I thank Chris Heyes, Transboundary Air Pollution project at IIASA, for guiding me through this investigation with many helpful suggestions, fruitful discussions, and much encouragement, not to mention the editorial work needed to put this report into its final form. I am also grateful to Markus Amann and Wolfgang Schöpp, Transboundary Air Pollution project at IIASA, for their many comments and ideas about this study. I thank David Simpson, EMEP and IVL at Göteborg, Sweden, for his careful review of the work and detailed comments about the content of this report. Finally, I am indebted to Markus Amann and the other members of the Transboundary Air Pollution project at IIASA for giving me the opportunity to work with them.

Contents **Page**

1. INTRODUCTION

Surface ozone has been widely studied over the past 30 years because of its adverse effects on human health and the environment. Most importantly, ozone can cause the airways of the lungs to narrow leading to breathing difficulties (Seinfeld, 1986). Ozone also has been implicated as a major contributor to the forest decline in western Germany and in the damage to crops such as potatoes, tobacco, and oats (Prinz, 1988). One tool for studying cost-effective strategies for reducing ozone, and so these adverse effects, is an integrated assessment model for surface layer ozone exposure (IAM).

An IAM must include information about emissions of ozone precursors (NOx (NO + NO_2) and VOCs (Volatile Organic Compounds)), available control technology, abatement costs, transport of ozone, and environmental effects. In such a complex system, each portion must be simple but realistic so that the model is efficient and generally applicable. Recently, Heyes et al. (1996) developed a simplified model of ozone formation and transport for use in an IAM by using a regression surface to summarize some of the results of the EMEP Ozone Model (Simpson et al., 1995; Simpson, 1995; Simpson, 1993; Simpson, 1992). This statistical model, called the seasonal model, relates annual NOx and VOC emissions to mean ozone mixing ratios over a three- to six-month period. Ideally, as part of an IAM, the seasonal model will contribute to the process of determining the most cost-effective way of reducing NOx and VOC emissions to achieve tolerable surface ozone mixing ratios over Europe.

While the seasonal model explicitly uses information about emissions of NOx and VOCs (compounds which are important to the *photochemical* source of boundary layer ozone), it does not explicitly include indicators for another potentially important source of boundary layer ozone: entrainment of free tropospheric ozone and its precursors into the boundary layer. Recent studies suggest that the influence of the free troposphere on boundary layer ozone can be important. For example, ozone mixing ratios at some elevated sites that are within the boundary layer in the United States and Europe are strongly influenced by the transport of ozone from the free troposphere (Kley et al., 1994). Similarly, in an investigation of the links between surface ozone and atmospheric circulations over Europe, Davies et al. (1992) find correlations between daily surface ozone mixing ratios and a wind speed index. In the winter, high ozone mixing ratios are associated with high wind speeds, suggesting that vertical exchange increases boundary layer ozone mixing ratios. Also, Moody et al. (1995) show that entrainment of ozone-rich air following the passage of spring low pressure systems produces the highest ozone mixing ratios at Bermuda.

The free tropospheric source of boundary layer ozone should be implicitly included in the predictor equations of the seasonal model since the model was developed based on the data from full simulations of the EMEP Ozone Model which includes mechanisms for the exchange of air between the boundary layer and the free troposphere. However, the implicit effects are representative only of those conditions under which the EMEP Ozone Model was simulated: April through September, 1989 emissions, meteorology, and boundary conditions. While changes in European emissions can be handled explicitly in the seasonal model, changes in free tropospheric composition resulting from changes in local, continental, hemispheric, or global scale emissions cannot be accounted for in the model in its present

form. Therefore, the implicit free tropospheric effect currently in the seasonal model may not be consistent with any European emission changes simulated with the seasonal model.

Whether or not changes in European emissions determine the basic chemical state of the free troposphere has a number of implications for emission control strategies. For example, if the source of ozone and its precursors in the free troposphere over Europe is European emissions, then European NOx and VOC emission reductions will have a direct effect on free tropospheric ozone. Such a scenario would influence boundary layer ozone in two ways: 1.) by influencing boundary layer mixing ratios of ozone precursors and 2.) by influencing mixing ratios of free tropospheric ozone and its precursors which can be mixed into the boundary layer. On the other hand, if the mixing ratios of free tropospheric species are determined by emissions from another source region, the European reduction scenarios will be addressing only the *in situ* photochemical production; the free tropospheric component of the boundary layer ozone will be unaltered. In this case, emission reductions from other source areas, such as North America, would have to be considered to accurately predict boundary layer ozone mixing ratios with the seasonal model and so to implement the IAM with confidence.

Before the issues of source areas and spatial scales are addressed in the context of the seasonal model, however, it is necessary to study what effect the free troposphere has on boundary layer ozone as predicted by the EMEP Ozone Model, upon which the seasonal model is based. The EMEP Ozone Model is a one layer, column trajectory, Lagrangian model for photochemical oxidants designed to study the formation and distribution of boundary layer ozone over Europe. Every 2 hours, air parcels in the midst of 96-hour trajectories pick up emissions of SO_2, NOx, CO, and VOCs from the underlying grids. Distribution and removal of these and other species are determined by a mass balance approach which considers emissions, chemical reactions, dry and wet removal, and meteorological influences (Simpson, 1992).

In the EMEP model, the exchange of air between the boundary layer and the free troposphere is accomplished in two ways: 1.) mixed layer height adjustment and 2.) cloud venting. The 12 GMT mixing heights in the model are determined from radiosonde measurements and during a trajectory, a mass balance of convergence and divergence by using the 850 mb vertical velocity is implemented to calculate the Lagrangian changes in mixing height. After 24 hours, the computed mixing height is compared to the corresponding radiosonde observation. If the calculated height is less than the observed height, then air from the top boundary of the model is allowed to mix into the boundary layer, with the amount of air mixed into the boundary layer determined by the difference between the two heights. The second exchange mechanism is cloud venting which is included in the model by assuming a vertical velocity through the base of convective clouds of 1 meter per second. The total flux out of the boundary layer, then, is balanced by an equal amount of air from the top boundary of the model. The top boundary conditions for the model are, in essence, free tropospheric chemical conditions and so these exchange mechanisms bring free tropospheric species into the boundary layer for processing (Simpson, 1992).

The aim of this study is to determine whether or not boundary layer ozone mixing ratios are influenced significantly enough by these exchange processes in the EMEP Ozone Model to be explicitly included in the seasonal model. The influence of the exchange process is assessed by studying the sensitivity of boundary layer ozone to various free tropospheric

conditions. Simpson (1992) finds that for July 1985, boundary layer ozone mixing ratios as predicted by the EMEP Ozone Model are not very sensitive to reducing free tropospheric ozone by 20% and setting free tropospheric NOx and VOC mixing ratios to zero. However, these sensitivity studies are performed with a model version which does not include cloud venting which, in this same paper, is shown to be an important exchange mechanism. The present study is a more comprehensive examination of the sensitivity of boundary layer ozone to free tropospheric ozone and its precursors and uses a more recent version of the EMEP Ozone Model which includes parameterizations for both exchange processes. In the following section, the current chemical state of the lower free troposphere over Europe is reviewed. Note that the lower free troposphere is defined here as the atmosphere between the top of the boundary layer and 5 km. Sources, sinks, lifetimes, trends, and present mixing ratios for ozone and its precursors (NOx, VOCs, CO, and CH_4) are discussed. Also included in this section are suggestions for updating the current EMEP Ozone Model free tropospheric conditions. Next, the methodology and scenarios used in this study are discussed, followed by the presentation and discussion of the major findings. Finally, several existing models which can be used to determine mixing ratios and origin of free tropospheric ozone and its precursors over Europe are reviewed.

2. THE LOWER FREE TROPOSPHERE OVER EUROPE

In this section, the current chemical conditions of the lower free troposphere, primarily over Europe, are reviewed. Information is given about the sources, sinks, lifetimes, observed mixing ratios, and current mixing ratio trends of ozone and its precursors: carbon monoxide (CO), methane (CH_4), NOx, and VOCs. Note that the published data required for this discussion of the lower free troposphere is lacking in some instances. Therefore, some information about other portions of the troposphere is supplied to give the reader a general sense of the behavior of these compounds. Table I summarizes the findings of this section.

2.1. Ozone

Ozone in the lower free troposphere has two main sources: in situ photochemical production and stratospheric intrusion of ozone-rich air. A photochemical steady state environment for ozone is given by the following NOx-catalyzed reactions:

$$O(^3P) + O_2 + M \rightarrow O_3 \quad (1)$$

$$NO + O_3 \rightarrow NO_2 + O_2 \quad (2)$$

$$NO_2 + h\nu \rightarrow NO + O(^3P) \quad (3)$$

For ozone to accumulate, NO must be converted to NO_2 without consuming ozone. Typically, photochemical reactions involving CO, CH_4, and VOCs perform this task. The oxidation of CO can produce ozone if there is sufficient NOx available:

$$CO + OH + O_2 \rightarrow CO_2 + HO_2 \quad (4)$$

$$HO_2 + NO \rightarrow NO_2 + OH\,, \quad (5)$$

followed by reactions (3) and (1). In a low NOx environment, reaction (5) is replaced by:

$$HO_2 + O_3 \text{ --> } HO + 2O_2 \qquad (6)$$

which leads to a net destruction of ozone (Cox, 1988).

The oxidation of methane and VOCs by OH also may lead to a net production of ozone, given sufficient NOx, by the following reactions:

$$RH + OH \text{--> } R^* + H_2O \qquad (7)$$

$$R^* + O_2 \text{ --> } RO_2 \qquad (8)$$

$$RO_2 + NO \text{ --> } NO_2 + RO \qquad (9)$$

followed by reactions (3) and (1), where RH is a hydrocarbon, such as CH_4, R* is a radical such as CH_3, and RO_2 is a peroxy radical, such as CH_3O_2 (Logan, 1985).

As mentioned above, given sufficient NOx as a catalyst, these reactions can lead to the net production of ozone. For example, Logan et al. (1981) suggest that for each CO molecule oxidized, one ozone molecule is produced and for each CH_4 molecule oxidized, 3.5 ozone molecules can be produced. For some larger hydrocarbons such as pentane, the yield is 10 to 14 molecules of ozone (Singh et al., 1981). NOx-catalyzed reactions of CO and CH_4 to produce ozone are generally important in unpolluted, background environments (e.g., Seinfeld, 1986), while the NOx-VOCs system is usually associated with photochemical smog in polluted regions (e.g., Greenberg and Zimmerman, 1984).

The second source of tropospheric ozone is transport from the stratosphere. The most important and most studied mechanism of this transport is tropopause folding. A tropopause fold is a dynamic process that can occur during rapid development of powerful storm systems. Circulations develop around the jet stream in the middle and upper troposphere drawing ozone-rich stratospheric air into the troposphere. Irreversible mixing processes complete the transfer of ozone to the middle and upper troposphere from where the ozone can be mixed into the lower free troposphere (Vaughn, 1988). Dynamic and thermodynamic processes associated with cut-off lows and the subtropical jet streams have also been proposed as initiators of the transfer of stratospheric ozone to the troposphere (Allam and Tuck, 1984; Bamber et al., 1984; Hoskins et al., 1985).

Many studies have investigated the relative importance of *in situ* photochemical production and stratospheric intrusions on ozone levels in the troposphere. For example, by using a zonally-averaged climate model for transport and other meteorological parameters to study the influence of stratospheric ozone on tropospheric ozone levels, Follows and Austin (1992) determined that less than 10% of lower free tropospheric ozone originates in the stratosphere at all latitudes and all seasons. Similarly, Parrish et al. (1993), in a study of the influence of North American ozone pollution on the North Atlantic pollution levels, suggest that during the summer, the ozone budget in the lower troposphere over the North Atlantic is dominated by photochemical production.

While ozone in the lower free troposphere has two main sources, it has one main sink: photochemical destruction. The photochemical loss of ozone is often described in terms of the loss of odd oxygen, defined as the sum of O_3, $O(^1D)$, $O(^3P)$, and NO_2. These compounds are rapidly interconverted and so removal of any of these compounds results in the loss of ozone. Reaction (6) above is one loss mechanism, as are the following reactions:

$$O(^1D) + H_2O \rightarrow 2HO \quad (10)$$

$$HO + O_3 \rightarrow HO_2 + O_2 \quad (11)$$

$$HO + NO_2 + M \rightarrow HNO_3 + M . \quad (12)$$

Because of the seasonal variations of this sink and the sources discussed above, the lifetime of ozone also varies seasonally. In the lower free troposphere, ozone has a lifetime of approximately two weeks during the summer, while during the winter, its lifetime is at least 200 days (Liu et al., 1987).

Many studies of lower free tropospheric ozone mixing ratios over Europe, whether performed by using balloons, elevated measurement sites, or aircraft observations, have revealed consistent features. For example, in the lower free troposphere (850 mb to 700 mb) during the 1980's, ozone mixing ratios reach a maximum of approximately 50 ppb to 55 ppb during the late spring and summer (e.g., Logan, 1985; Bojkov, 1988; Marenco and Said, 1989; Beekman et al., 1994). Peaks greater than 100 ppb have been observed and are attributed to either local photochemical production or stratospheric intrusions (Marenco and Said, 1989). Minimum free tropospheric mixing ratios are observed in the winter (December and January), with values of approximately 35 ppb to 40 ppb. The standard deviation for the winter mixing ratios is roughly 1 ppb, while that for the summer mixing ratios is 8 ppb (Logan, 1985; Beekman et al., 1994).

In addition to temporal variations, spatial variations of ozone have been observed across Europe. Logan (1985) finds that ozone at 700 mb peaks between 48° N and 53° N and is mainly the result of photochemical reactions of anthropogenic ozone precursors. Similarly, Beekman et al. (1994) find more middle troposphere ozone at 51° N than at 44° N over the period of 1984 through 1990.

Observations suggest that lower free tropospheric mixing ratios of ozone have increased over the past century. For example, ozone mixing ratios in 1934 over Arosa, Switzerland at 3450 m were approximately 30 ppb, while those over Hohenpeissenberg, Germany at this altitude in 1984 were roughly 60 ppb. More specifically, over Hohenpeissenberg, from 850 mb to 500 mb, ozone increased approximately 2% per year from the late 1960's to the early 1980's (Logan 1985; Bojkov, 1988). An increase of 1.6% per year was observed over a similar period at 800 mb above Payerne, Switzerland (Staehelin and Schmid, 1991). More recent data presented by Sladkovic et al. (1994) suggest that the growth rate of ozone between one and three kilometers is approximately zero over southern Switzerland at present. They do note, however, that over the period of observation (16 years for one site and 5 years for another) there is a general increasing trend.

The growth rates vary depending on the time of the year and altitude, as well. For example, Bojkov (1988) notes that while the observed increases in ozone over Hohenpeissenberg occur in all seasons and in the lowest 75% of the free troposphere, they are

largest from November through January in the lower free troposphere and smallest from May through October. These growth rates are in contrast to those found by Sladkovic et al. (1994) which showed maximum and minimum growth rates in August and October, respectively. In addition, a shift in the summer maxima from May and June toward June and July has been observed (Bojkov, 1988).

2.2. Carbon Monoxide

Carbon monoxide is a major constituent of tropospheric chemistry. It is the major sink for OH, the main oxidant in the atmosphere (reaction (4)), and, as discussed previously, reactions involving CO may lead to a net production or destruction of ozone, depending on the level of NOx (reactions (4), (5), and (6)). The major CO sources are fossil fuel consumption, biomass burning, oxidation of VOCs, and the oxidation of CH_4 (Novelli et al., 1994). Each of these sources contributes approximately equally to the total CO emission rate, half of which is from anthropogenic activity (Khalil and Rasmussen, 1994). CO is removed from the atmosphere by reaction with OH (90% to 95% of the sink), by loss to the stratosphere, and by oxidation via biological consumption in soils (Logan et al., 1981). The combination of sources and sinks gives CO a lifetime of approximately two to three months in the lower troposphere.

During the 1980's, several studies suggested that background mixing ratios of CO were increasing at roughly 1% per year (Zander et al., 1989; Khalil and Rasmussen, 1988). More recent studies suggest that the levels of atmospheric CO have decreased over the past several years. For example, Novelli et al. (1994), by examining measurements at 27 locations across the globe, find that in the northern hemisphere, CO has decreased 6.1% per year or 7.3 ppb per year from June 1990 to June 1993. On a global basis, Khalil and Rasmussen (1994) find a rate of decrease of 2.6% per year from 1988 through 1992. The decrease may be caused by a combination of the following: 1.) a decrease in USA and European emissions due to strict controls on automobile CO emissions and 2.) an increase in the OH mixing ratio, a major sink of CO (Prinn et al., 1992; Bakwin et al., 1994; Bekki et al., 1994).

Currently in the lower free troposphere, CO mixing ratios are highest in the late winter and early spring (up to 230 ppb) when OH is at a minimum and are at a minimum during the summer (as low as 60 ppb). Average mid-latitude seasonal oscillations of CO mixing ratios are roughly 50 ppb to 100 ppb (Novelli et al., 1992; Novelli et al., 1994). In addition, mixing ratios decrease from north to south and from polluted, continental areas toward clean, oceanic areas (Novelli et al., 1994). During June 1984, CO mixing ratios over western Europe were measured at between 150 ppb and 180 ppb at 2 to 3 kilometers (Marenco et al., 1989). Marenco et al. suggest that the range of free tropospheric CO mixing ratios is typically from 100 ppb to 200 ppb over the continental northern hemisphere (NH), while those over the oceanic NH are between 80 ppb and 90 ppb.

2.3. Methane

As discussed above, methane plays an important role in tropospheric chemistry by influencing ozone and OH. In addition, methane absorbs infrared radiation and so is a contributor to the greenhouse effect. The most significant single source of atmospheric methane is methanogenesis from wetland habitats. Anthropogenic sources such as biomass burning and natural gas leakage are also important to the total methane emission rate. Reaction with OH is the largest sink of atmospheric methane, although consumption by

aerobic bacteria also contributes. These sources and sinks give methane a lifetime of approximately 10 years (Schlesinger, 1990; Dlugokencky et al., 1994). This long lifetime implies that methane is evenly distributed throughout the troposphere.

The atmospheric mixing ratios of atmospheric methane have been increasing for about two centuries for reasons that are not completely understood (Schlesinger, 1990). One possibility is that increased CO mixing ratios may sequester OH radicals, removing the most important sink of methane. During the 1980's and the early 1990's the rate of increase decreased from ~14 ppb per year to ~9 ppb per year (WMO, 1992). The growth rate was near zero during 1992, perhaps due to decreased emissions from the former Soviet Union and eastern Europe (Dlugokencky et al., 1994) On the other hand, the decreased rate may have been due to a large stratospheric ozone depletion in 1991 and 1992, which could have resulted in increased OH mixing ratios (Bekki et al., 1994).

As of 1992, northern hemispheric methane mixing ratios exhibited a slight north to south gradient ranging from approximately 1750 ppb at 20° N to 1780 ppb at 45° N to 1825 ppb at 65° N (Dlugokencky et al., 1994). Vertically, the methane mixing ratios decreased by about 1% from the surface to 3400 m at one station over the island of Hawaii. A complicated seasonal variation of methane occurred in the northern hemisphere with an amplitude of between 40 ppb and 60 ppb.

2.4. Nitrogen compounds

Like methane, nitrogen compounds such as NO, NO_2, PAN, and HNO_3 influence the mixing ratios of OH and ozone. Most of the nitrogen species are formed from the initial release of NOx (NO + NO_2) whose largest source is fossil fuel consumption. Other important sources include lightning, microbial activity in soils, aircraft emissions, injection from the stratosphere, and oxidation of ammonia. Anthropogenic sources represent approximately 60% of the total NOx emission mass, although estimated source strengths have a wide range (Logan, 1983; Liu and Cicerone, 1984). The sinks of NOx include removal in precipitation, dry deposition, conversion of NO_2 to HNO_3 (reaction (12)), or conversion to particulate nitrate followed by heterogeneous removal (Fehsenfeld et al., 1988).

Because of large spatial and temporal nonuniformities in NOx sources and sinks, NOx exhibits a large range of lifetimes depending on location and time of year. Liu et al. (1987) suggest that during the summer the lifetime of NOx in the boundary layer is between 0.5 days and one day, depending on the level of NOx. During the summer, the lifetime is controlled by the reaction of NO_2 with OH (reaction (12)). The wintertime lifetime is much more uncertain but is probably on the order of one week (Liu et al., 1987). Due to smaller OH mixing ratios in the lower free troposphere, the lifetime of NOx in the lower free troposphere is expected to be longer than these boundary layer values.

NOx mixing ratios in the northern hemisphere, lower free troposphere generally range from 0.2 ppb in more remote areas to 5 ppb over the most polluted areas, with a wide variability of values (Fehsenfeld et al., 1988; Vögtlin et al., 1994). NO mixing ratios, which are generally much smaller than the NO_2 mixing ratios, vary from 0.02 ppb to 0.13 ppb in the lower free troposphere over continental western Europe, especially away from sources (Drummond et al., 1988). Measurements of NO and NO_2 at about 2.5 km over northwest

Turkey show, respectively, mixing ratio ranges of 0.17 ppb to 0.41 ppb and 0.23 ppb to 2.7 ppb (Baykal et al., 1994). NOx mixing ratios also exhibit a slight seasonal cycle with maximum values in the winter and minimum values in the summer, due to the seasonal variation of NOx sinks. Current trends in NOx mixing ratios, if any, have not been determined.

It is important to note that NOx mixing ratios in the free troposphere can be significantly influenced by the formation of peroxyacetyl nitrate (PAN). PAN is formed during the oxidation of VOCs and is a temporary reservoir of NOx, especially in colder areas (Singh et al., 1985). Therefore, PAN may be transported over large distances and then can thermally dissociate, resulting in the long-range transport of NO_2. Lower free tropospheric mixing ratios of PAN over western Europe have been measured in the range of 10 ppt to 170 ppt (Rudolph et al., 1987). Oceanic values measured on the Canary Islands vary from less than 10 ppt to about 70 ppt (Schmitt, 1994). Singh et al. (1992) report mixing ratios over the western Atlantic Ocean of between 100 ppt and 500 ppt.

2.5. Volatile organic compounds

As discussed above, VOCs indirectly can lead to the production of ozone. In addition, these compounds have adverse direct effects because many of them are toxic, mutagenic, and/or carcinogenic (Duce et al., 1983). Three of the most abundant VOCs in the free troposphere are ethane (C_2H_6), ethene (C_2H_4), and n-butane (n-C_4H_{10}) and the following discussion will focus primarily on these species.

The dominant anthropogenic sources of VOCs are the combustion of fossil fuels, evaporation of fossil fuels and solvents, and industrial processes (Field et al., 1992). The hydrocarbons emitted by these sources are generally alkanes, alkenes, and aromatics in the C1 to C10 range (Hov et al., 1989). The largest natural source of ethane and n-butane is the seepage of natural gas as a result of bacterial fermentation, while the natural sources for ethene include fruits, flowers, roots, and tubers (Altshuller, 1983). The dominant removal mechanism of these species is photochemical oxidation primarily by OH, O_3, and NO_3, while wet and dry deposition are generally minor removal mechanisms.

Because of a wide range of reactivities and source characteristics in the atmosphere, the lifetimes of VOCs vary from several hours to several months. For example, ethane, n-butane, and ethene have respective lifetimes of two to three months, seven to ten days, and three days based on OH mixing ratios of $7x10^5$ molecules-cm^{-3} and O_3 mixing ratios of 30 ppb (Field et al., 1992).

As expected from the wide range of lifetimes and large variability of sources, the composition and mixing ratios of VOCs in the lower troposphere are highly variable. In general, ethane, due to its long lifetime, is the most abundant VOC in the atmosphere with mixing ratios roughly between 1 ppb and 5 ppb, averaging about 2 ppb (Singh et al., 1988; Rudolph, 1988; Lightman et al., 1990; Penkett et al., 1993; Rudolph, 1995; Schmitt and Carretero, 1995). Ethene and n-butane have mixing ratios of between 0.1 and 1 ppb in the lower free troposphere over western Europe and the eastern North Atlantic (Tille et al., 1985; Rudolph, 1988; Kanakidou et al., 1989; Lightman et al., 1990; Penkett et al., 1993; Schmitt and Carretero, 1995). Ethane, n-butane, and ethene show maximum values during the winter and minimum values during the summer over western Europe and the eastern North Atlantic

(Tille et al., 1985; Penkett et al., 1993; Schmitt and Carretero, 1995). The day-to-day variability of these species ranges from near 5% for ethane to more than 30% for n-butane and ethane (Lightman et al., 1990; Schmitt and Carretero, 1995).

Table I. Likely continental, summer and winter mixing ratios (45°N) and lifetimes of ozone and its precursors in the lower free troposphere over Europe, as determined from published studies. The letters in parentheses refer to the list of references beneath the table. Where possible, a distinction between oceanic and continental locations is given.

Species	Summer				Winter			
	Mixing ratio (ppb)		Lifetime		Mixing ratio (ppb)		Lifetime	
Ozone	50 to 55	(a)	14 days	(b)	35 to 40	(c)	> 200 days	(b)
CO			80 days	(d)			>80 days	(d)
Continental	100 to 150	(d)			180 to 230	(d)		
Oceanic	50 to 100	(d)			>80	(d)		
CH_4	1780	(e)	10 years	(f)	1780	(e)	10 years	(f)
NOx			>0.5 days	(b)			>7 days	(b)
NO	0.01 to 0.2	(g)			0.01 to 0.2	(g)		
NO_2	0.2 to 5	(g)			0.2 to 5	(g)		
VOCs								
Ethane	1 to 5	(h)	60 days	(i)	2 to 5	(h)	> 60 days	(i)
Ethene	0.1 to 1	(h)	3 days	(i)	0.2 to 1	(h)	> 3 days	(i)
n-Butane	0.1 to 0.7	(h)	3 days	(i)	0.2 to 0.8	(h)	> 3 days	(i)

a: Logan (1985); Marenco and Said (1989); Bojkov (1988); Beekman et al. (1994).
b: Liu et al. (1987).
c: Logan (1985); Beekman et al. (1994).
d: Marenco et al. (1989); Novelli et al. (1992); Novelli et al. (1994).
e: Dlugokencky et al. (1994).
f: Schlesinger (1990), Dlugokencky et al. (1994).
g: Fehsenfeld et al. (1988); Drummond et al. (1988); Vögtlin et al. (1994); Baykal et al. (1994).
h: Ehhalt et al. (1985); Tille et al. (1985); Rudolph et al. (1987); Rudolph (1988); Kanakidou et al. (1989); Lightman et al. (1990); Field et al. (1992); Penkett et al. (1993); Rudolph (1995).
i: Field et al. (1992).

2.6. EMEP Ozone Model free tropospheric conditions

As discussed previously, the EMEP Ozone Model allows for the exchange of air between the free troposphere and the boundary layer due to mixed layer growth and cloud venting. In general, the free tropospheric mixing ratios as currently set in the model vary depending on latitude, month, and geographical location (i.e., oceanic or continental grids). Table II lists the base free tropospheric mixing ratios of the background species for

continental and oceanic grids, while respectively, Figure 1 and Figure 2 graphically represent the scaling factors used to determine the latitudinal and monthly variations from these base conditions for some selected species. Ozone is at its maximum at 40° N and during May and June and is at its minimum at 70° N and during September. Maximum PAN mixing ratios are found in May at 50° N, while minimum mixing ratios are found in September and at 70° N. NO and NO_2 mixing ratios in the model have no seasonal variation, but do have a latitudinal variation with a maximum at 50° N. The free tropospheric VOCs in the model vary seasonally, with a maximum in April (not shown) and have no latitudinal variations. Finally, oceanic ozone values are 20% lower than the continental ozone mixing ratio at a given latitude.

Table II. The base mixing ratios of free tropospheric species (in ppb) as set in the EMEP Ozone Model for continental grids, oceanic grids, and for all grids, where appropriate. Latitudinal and monthly scaling factors (given in Figures 1 and 2 for selected species) are applied to these base mixing ratios. The values in parentheses are suggested mixing ratios based on a literature review. See text for details.

Species	**Continental (ppb)**		**Oceanic (ppb)**	
Ozone	50	(c)	a	
NO	0.5	(0.15)	0.05	
NO_2	0.5	(1.0)	0.05	
HNO_3	0.3		0.1	
SO_2	1.0		0.1	
HCHO	0.25		0.25	
PAN	0.35	(0.25)	0.35	(0.1)
	All Grids (ppb)			
CH_4	1500		(1780)	
H_2	500			
CO	200		(oceanic: 80; continental: 150)	
Sulfate Aerosols	0.08			
C_2H_6[&]	2			
C_2H_4[$]	0.2			
C_4H_{10}[#]	2			
NO_3	0.001			
N_2O_5	0.001			
Nitrate	b			

a: Oceanic ozone values are set to 80% of the continental value at a given latitude
b: Nitrate mixing ratios are set equal to the HNO_3 mixing ratios
c: Limited data suggests that monthly maximum ozone should be shifted to June and July from May and June
&: Includes ethane, acetylene, benzaldehyde, acetone, and trichloroethylene
$: Includes ethene, butylene, 2-methylbut-1-ene, 3-methylbut-1-ene, and 2-methylbut-2-ene
#: Includes n-butane, 2methylpentan-4-one, cyclohexanone, and all other alkanes except ethane and methane

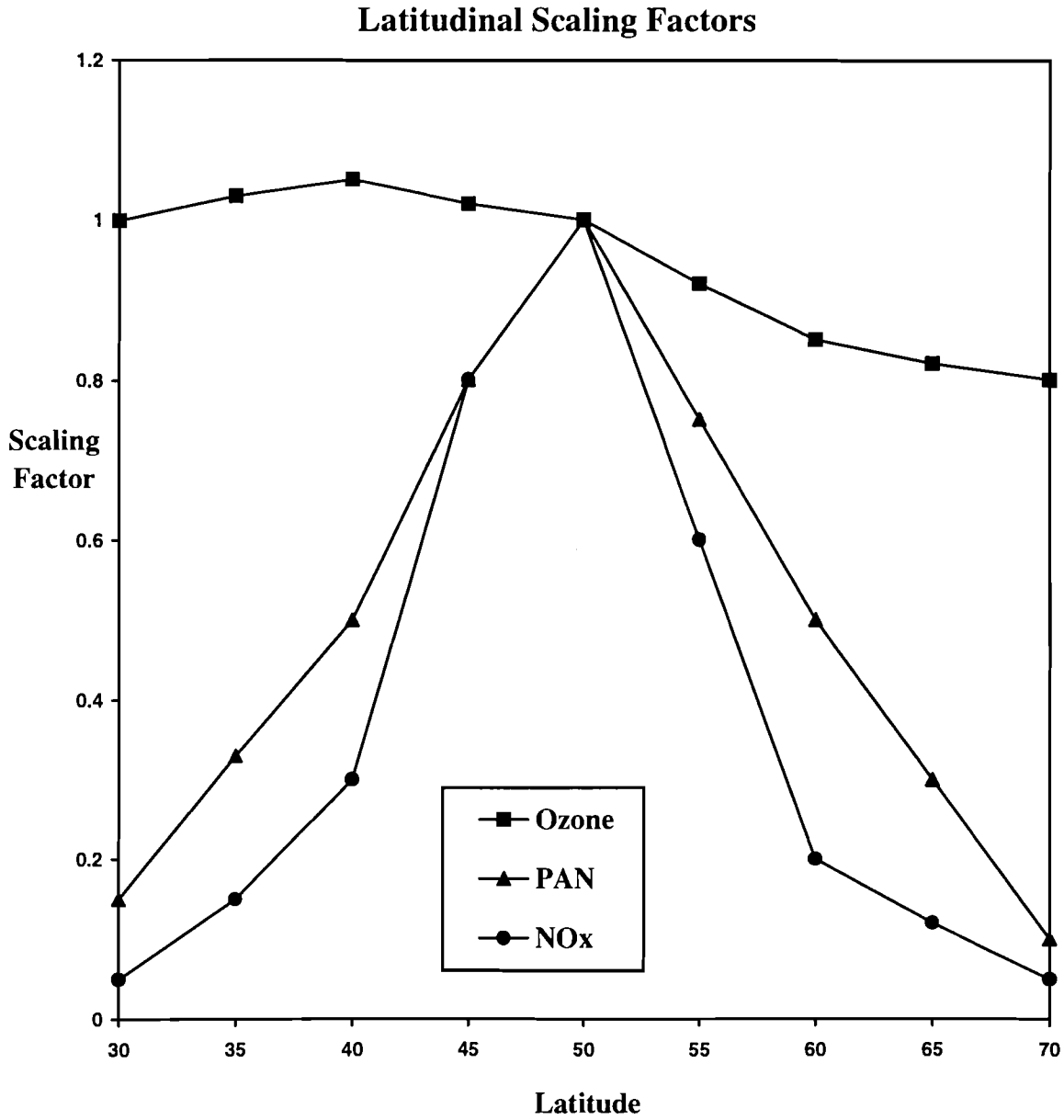

Figure 1. The scaling factors used for determining the latitudinal variations in free tropospheric ozone, NOx and PAN as set in the EMEP Ozone Model. These scaling factors are applied to the base mixing ratios given in Table II.

Based on the literature review presented above, it is suggested that the free tropospheric mixing ratios of some species in the EMEP Ozone Model be updated. The suggested mixing ratios are given in parentheses in Table II. The continental mixing ratios of NO should be lowered to 0.15 ppb while that of NO_2 should be increased to about 1.0 ppb. These values represent averages of mixing ratios given by Fehsenfeld et al. (1988), Drummond et al. (1988), and Vögtlin et al. (1994). Data collected by Rudolph et al. (1987) suggest that the free tropospheric continental mixing ratio of PAN in the EMEP model is too high. However, PAN measurements are sparse. So until more PAN data is available, it is suggested that free tropospheric PAN mixing ratios be reduced only slightly. Oceanic values of PAN, as measured by Penkett et al. (1993), Schmitt (1994), Schmitt and Carretero (1995)

suggest that oceanic PAN mixing ratios vary greatly with an average value of about 0.1 ppb. Therefore, it is suggested that the EMEP, free tropospheric, oceanic PAN mixing ratio be lowered to 0.1 ppb. The methane mixing ratios over all grids should be increased to 1780 ppb, which is a value suggested by Dlugokencky et al. (1994). Novelli et al. (1992) and Marenco et al. (1989) show that carbon monoxide mixing ratios are lower over the Atlantic Ocean than those over continental Europe. The EMEP free tropospheric CO mixing ratios should be changed to represent this land-sea contrast with oceanic values of 80 ppb and continental values of 150 ppb. Current free tropospheric mixing ratios of VOCs in the EMEP model are reasonable. Although not seen at all stations, the occurrence of maximum ozone mixing ratios has been observed to shift from late spring to the summer (Bojkov, 1988). Such a shift should be considered for the EMEP model's free tropospheric ozone mixing ratios. In the absence of data to the contrary, the specified monthly and latitudinal variations of the other species are reasonable. The influence of these suggested changes on the ozone predictions of the EMEP model are discussed in the section 3.8.

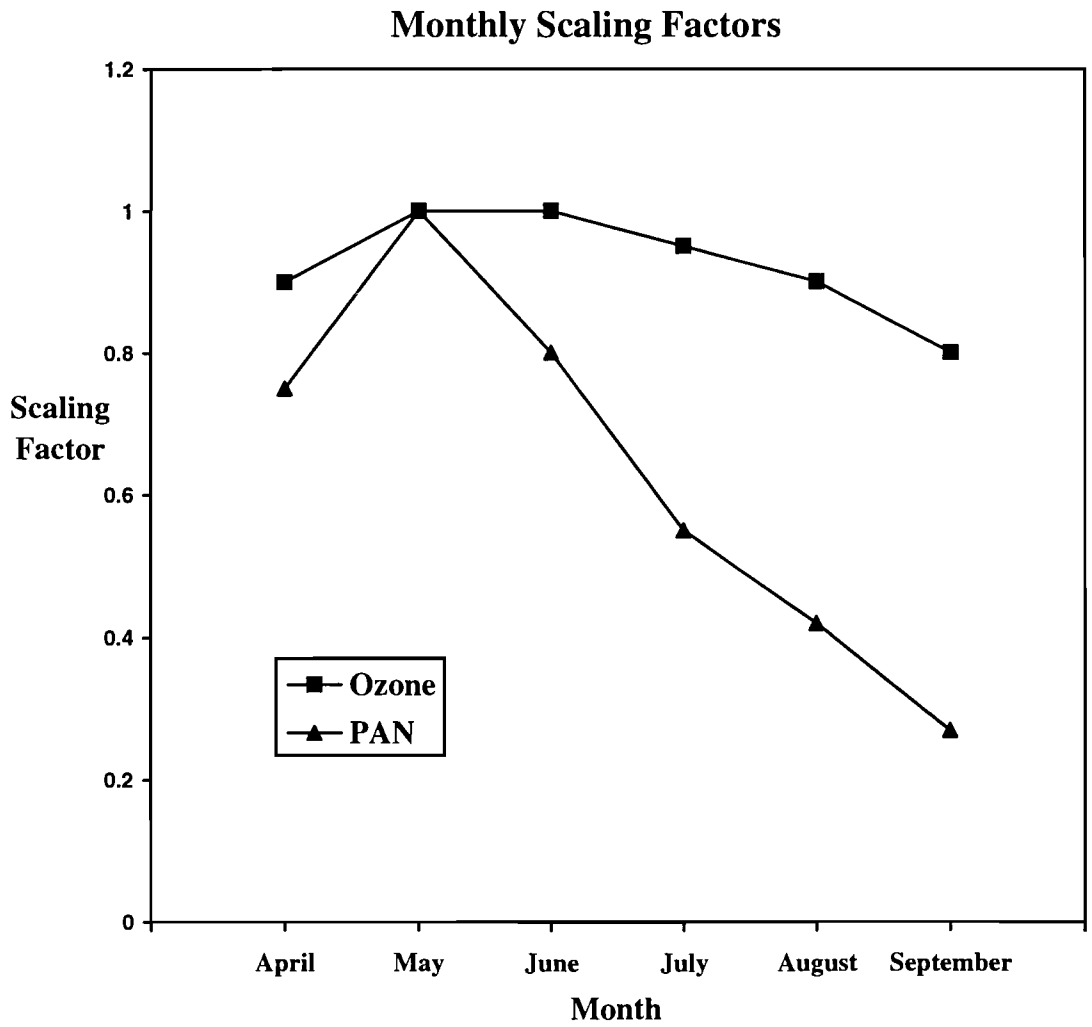

Figure 2. The scaling factors used for determining the monthly variations in free tropospheric ozone and PAN as set in the EMEP Ozone Model. These scaling factors are applied to the base mixing ratios given in Table II.

3. RESULTS

3.1. Methodology

To determine the influence of the free troposphere on the boundary layer average ozone mixing ratios as determined by the EMEP Ozone Model, the results of a base case model run with no changes in the free tropospheric conditions are compared to results obtained by varying the free tropospheric boundary conditions. The scenarios investigated in this study are listed in Table III. All free tropospheric mixing ratios are reduced and increased by 50% and individual species groups are separately increased and decreased by 50% to determine which free tropospheric species have the greatest influence on boundary layer ozone mixing ratios. The species are divided into three groups: 1.) Ozone, 2.) Nitrogen species, including NO, NO_2, HNO_3, PAN, NO_3, N_2O_5, and nitrate, and 3.) Carbon species, including CH_4, CO, HCHO, C_2H_6, C_2H_4, and n-C_4H_{10}. Note that the last three carbon species represent the sum of several species, as shown in Table II.

Table III. The various scenarios of the free tropospheric conditions examined in this study. The "carbon species" include CH_4, CO, HCHO, C_2H_6#, C_2H_4#, and n-C_4H_{10}#. The "nitrogen species" include NO, NO_2, HNO_3, PAN, NO_3, N_2O_5, and nitrate.

Scenario	Free Tropospheric Perturbation
Base case	No changes in the EMEP Ozone Model free tropospheric mixing ratios
1	Reduce all free tropospheric species by 50%
2	Reduce only ozone by 50%
3	Reduce only the nitrogen species by 50%
4	Reduce only the carbon species by 50%
5	Increase all free tropospheric species by 50%
6	Increase only ozone by 50%
7	Increase only the nitrogen species by 50%
8	Increase only the carbon species by 50%

#: In the EMEP model, these species represent a combination of several species. See Table II for details.

To put the 50% changes into perspective, free tropospheric ozone mixing ratios vary by about 20% from day to day in the summer (Logan, 1985; Beekman et al., 1994) with occasional day-to-day variations of up to 100% (Marenco and Said, 1989; Kley et al., 1994). Some VOCs have shown day-to-day variations greater than 30% (Lightman et al., 1990; Schmitt and Carretero, 1995).

Absolute and relative differences between the base case and the perturbation case daily, 12 GMT ozone mixing ratios for the period of April through September, 1989, are computed, as are standard deviations of these differences. The 12 GMT mixing ratios represent early afternoon values across this domain. Note that for this portion of the study the

"free tropospheric conditions" refer to the original free tropospheric values in the EMEP model, not the suggested modifications.

Data from fifteen grids in the EMEP domain are analyzed. The fifteen grid locations are listed in Table IV and are indicated in Figure 3. These sites are chosen to represent the wide range of meteorological and chemical conditions which occur in the EMEP domain. Note that the selected fifteen grids include areas with an expected marine influence and those with an expected continental influence.

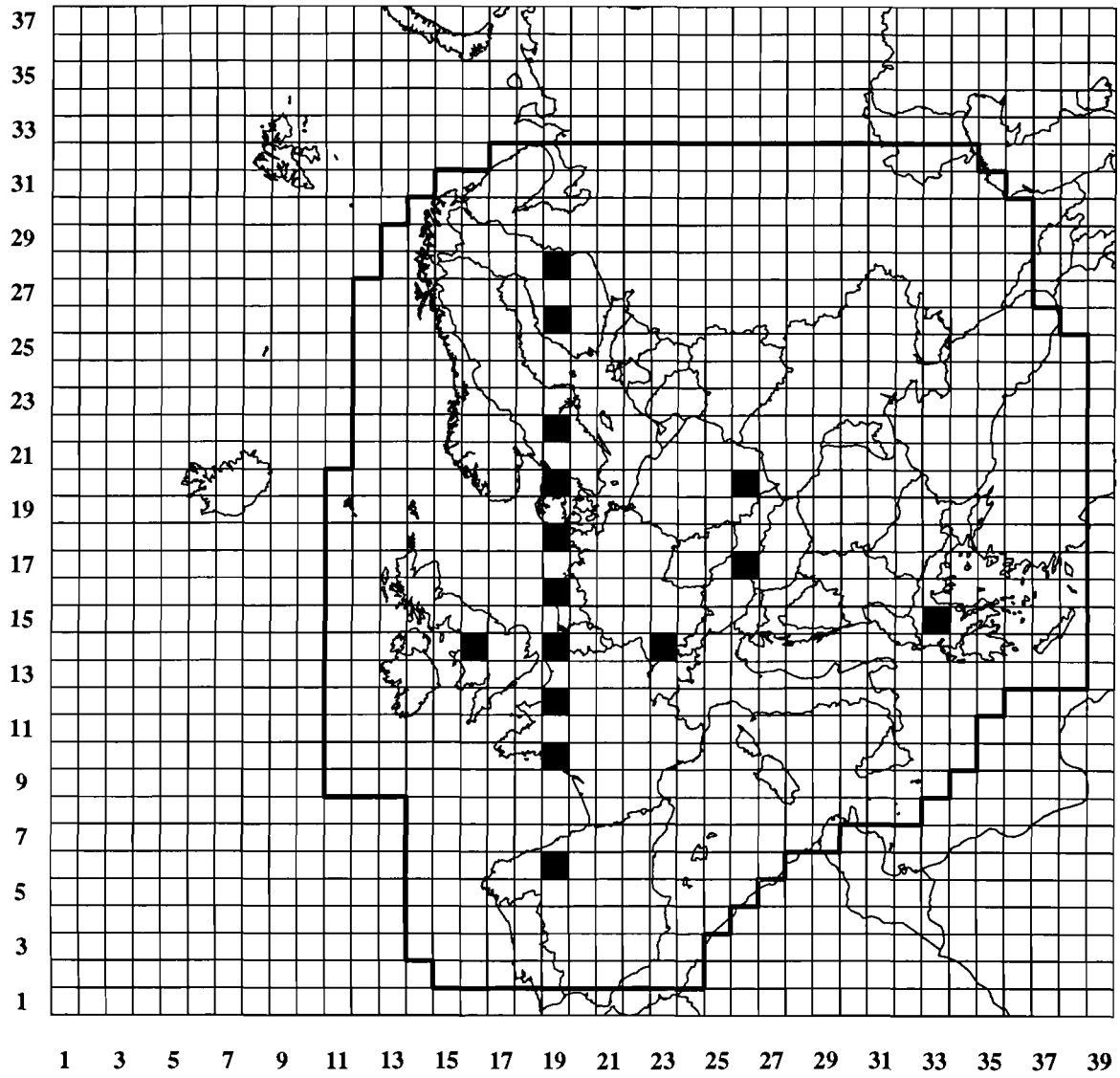

Figure 3. The EMEP Ozone Model domain. Filled grid squares indicate those grids examined in this study.

Table IV. The region, site abbreviation, and EMEP grid location of the fifteen sites used in this study.

Region/Location	Site name	Grid Location	
		x	y
Continental			
Schauinsland	DE03	23	14
Eastern Austria	AT67	26	17
Southeast Poland	PL60	26	20
Marine			
Northern Spain	SP06	19	06
Western France	FR10	19	10
Northern France	FR12	19	12
Belgium/France	BE14	19	14
Northern Netherlands	NL16	19	16
Southern Denmark	DK18	19	18
Northern Denmark	DK20	19	20
Central Sweden	SE22	19	22
Western Finland	SF26	19	26
Eastern Finland	SF28	19	28
Northwest England	UK64	16	14
Greece	GR35	33	15

3.2. Six-month-average boundary layer ozone responses

Table V lists the absolute and relative differences found by comparing the boundary layer ozone values of the base case and those of the perturbation cases, averaged over the model run and over all fifteen sites. Scenarios 5 through 8 are cases where the free tropospheric conditions are somehow increased (refer to Table III).

Table V. Absolute and relative differences between the base case EMEP boundary layer ozone predictions and the perturbation values. Standard deviations are given in parentheses after each value.

Scenario	Absolute Difference (ppb)		Relative Difference (%)	
1	-18.9	(5.1)	-35	(11)
2	-13.4	(4.5)	-24	(11)
3	-1.3	(0.7)	-3	(2)
4	-4.0	(2.3)	-7	(4)
5	17.8	(4.5)	32	(12)
6	13.3	(4.3)	24	(11)
7	1.1	(0.7)	2	(1)
8	3.2	(1.9)	6	(3)

When all the background conditions are increased by 50% (scenario 5), the boundary layer ozone mixing ratios increase by an average of 18 ppb from the base case average ozone mixing ratio of 55 ppb. The boundary layer ozone response to 50% increases in individual groups of species, as shown in Table V, indicates that boundary layer ozone is most sensitive to free tropospheric changes in ozone. A 50% increase in free tropospheric ozone leads to a 24% increase in boundary layer ozone, while the percentage increase for the nitrogen and carbon perturbations are much smaller with values of 2% and 6%, respectively. The magnitudes of the standard deviations given in Table V indicate that the variability around these values is not very large. The results from scenarios 1 through 4 in which free tropospheric mixing ratios are reduced by 50% are very similar in magnitude but opposite in sign to those obtained from the cases in which mixing ratios are increased. It is interesting to note that the boundary layer ozone response obtained from changing all background species by 50% (scenarios 1 and 5) is almost identical to the sum of the responses obtained from changing individual groups of species (scenarios 2 through 4 and 6 through 8, respectively).

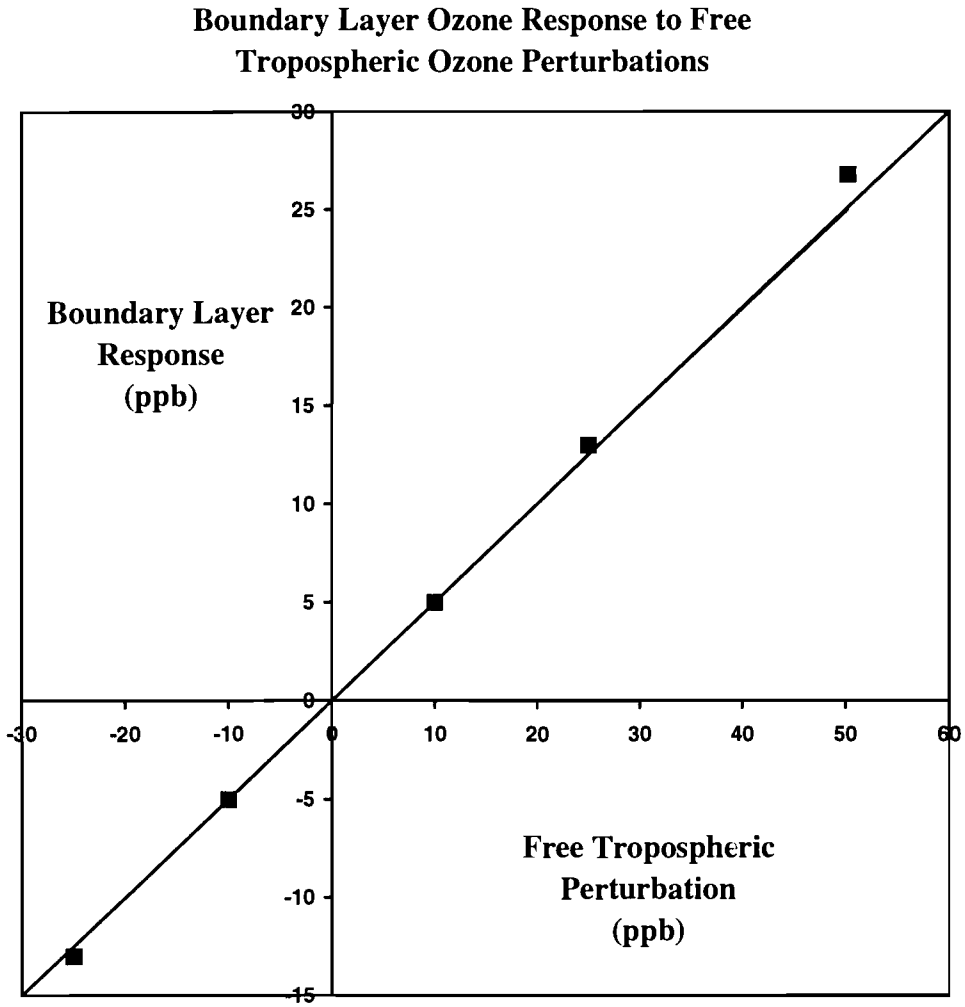

Figure 4. The boundary layer ozone response to various perturbations of free tropospheric mixing ratios of ozone. Black squares indicate the average response (perturbation case minus base case) over all fifteen sites and over the six month model period. The solid black line is a line of slope 0.5 for reference.

Plotted in Figure 4 are boundary layer ozone responses to changes in free tropospheric ozone mixing ratios. The data in this figure include those results from scenario 2 and scenario 6 in which free tropospheric ozone is changed by 50%, as well as the results from model runs in which the free tropospheric ozone mixing ratios are increased by 100%, increased by 20%, and decreased by 20% (not shown previously). In general, the boundary layer ozone response is about 50% of the free tropospheric perturbation. Slight deviations from this observation can be seen when the data points are compared to the line with a slope of 0.5 that is also plotted on this graph.

3.3. Responses of other boundary layer species to increased free tropospheric ozone

In this section, the chemical changes in the boundary layer that result when free tropospheric ozone is increased by 50% (scenario 6) are examined. Table VI presents a comparison of the mixing ratios of various boundary layer species averaged over all cases and over all six months for the base case and for the case in which free tropospheric ozone is increased by 50%.

Table VI. Changes in boundary layer mixing ratios of several species when the free tropospheric mixing ratios of ozone are increased by 50%.

Species	Mixing Ratio		Relative Change
	Base Case	Perturbation Case	
O_3	55 ppb	68 ppb	+24%
NO	0.5 ppb	0.4 ppb	-20%
NO_2	1.2 ppb	1.1 ppb	-8%
PAN	0.66 ppb	0.75 ppb	+14%
HNO_3	0.80 ppb	0.83 ppb	+4%
H_2O_2	0.49 ppb	0.61 ppb	+24%
OH	0.27 ppt	0.28 ppt	+4%
HO_2	16 ppt	18 ppt	+13%
RO_2	6.0 ppt	8.0 ppt	+33%

It is clear from Table VI that the increased ozone from the free troposphere leads to chemical changes in the boundary layer. For example, NOx mixing ratios decrease, mostly due to the loss of NO. In addition, HO_2, H_2O_2, PAN, and RO_2 (includes all peroxy radicals except HO_2) show substantial increases. These changes can be explained as follows:

When more ozone is mixed into the boundary layer, more OH radicals are produced by the following reaction:

$$O_3 + h\nu\ (+H_2O) \rightarrow 2OH + O_2\ . \qquad (13)$$

The excess OH radicals attack hydrocarbons producing RO_2:

$$RH + OH\ (+O_2) \rightarrow RO_2 + H_2O\ . \qquad (14)$$

The RO_2 then react with NO or NO_2:

$$RO_2 + NO\ (+O_2) \rightarrow NO_2 + HO_2 + RCHO \qquad (15)$$

$$RO_2 + NO_2 \rightarrow PAN\ . \qquad (16)$$

In reaction (16), NOx is stored. The HO_2 radicals produced during the above reactions react to produce H_2O_2:

$$HO_2 + HO_2 \rightarrow H_2O_2 + O_2\ . \qquad (17)$$

Finally, OH and NO_2 react to remove NOx:

$$NO_2 + OH \rightarrow HNO_3\ . \qquad (18)$$

The decreased NOx, then, is explained by the increase in PAN and HNO_3, while the increases in H_2O_2, HO_2, and RO_2 result from the increased production of free radicals and subsequent oxidation. Moreover, if the oxidizing capacity of the boundary layer is defined as the sum of O_3, OH, and H_2O_2 (Thompson, 1992), then the oxidizing capacity of the boundary layer increases due to the increased free tropospheric ozone.

3.4. Explaining the boundary layer ozone responses

One issue which has yet to be addressed is the reason for the boundary layer ozone increase when free tropospheric ozone increases. There are two possibilities: 1.) mixing of greater amounts of ozone into the boundary layer directly increases the ozone mixing ratios and 2.) subsequent chemical production of ozone following the exchange between the free troposphere and the boundary layer leads to increased ozone mixing ratios. The previous section shows that the increased free tropospheric ozone produces large changes in the chemical state of the boundary layer. But as the following analysis shows, the direct mixing of ozone from the free troposphere into the boundary layer is the main cause of the boundary layer ozone response due to 50% increases in free tropospheric ozone mixing ratios.

The chemical evolution of boundary layer ozone is examined over each two-hour interval of each trajectory ending at 12 GMT for intervals in which exchange occurs and for intervals when no exchange occurs. At the beginning of each two-hour trajectory interval, the model determines whether or not exchange will occur. If exchange is predicted to occur, the effect of the mixing is incorporated immediately, followed by two hours of chemistry at 15-minute intervals. If no exchange is predicted, chemistry begins at once.

In this analysis, when there is exchange, the effect of the mixing process on the boundary layer ozone mixing ratios at the time of the exchange is determined first. Specifically, the following question is addressed: at the moment when exchange occurs, do the boundary layer ozone mixing ratios increase or decrease? The contribution of free tropospheric ozone to the new boundary layer ozone mixing ratios (after mixing, but before chemistry) is computed. The net ozone production rate (photochemical production + photochemical loss + dry deposition loss) is computed over the two-hour period after the mixing has occurred. For each two-hour period during which no exchange occurs, the net

ozone production rate is determined as well. The results of this investigation, averaged over all cases and all six months, are presented in Table VII for the base case and the case in which the free tropospheric ozone is increased by 50%.

Table VII. A comparison of data for the Base Case and the case in which free tropospheric ozone is increased by 50% (Perturbation Case). The data is collected for each two-hour period of each trajectory ending at 12 GMT. The data are separated into groups for which exchange occurs at the beginning of the two-hour period and for which exchange does not occur. The data from each group are then averaged over all sites and all six months. The 'initial ozone mixing ratio' refers to the mixing ratio of ozone when chemistry begins. See text for details. (NA=Not Applicable)

	Base Case		**Perturbation Case**	
	Exchange	**No Exchange**	**Exchange**	**No Exchange**
Before Chemistry				
Ratio of ozone mixing ratio just after exchange to that just before exchange	0.99	NA	1.02	NA
Initial ozone mixing ratio	44.3 ppb	48.5 ppb	57.3 ppb	57.9 ppb
Boundary layer contribution to the initial ozone mixing ratio after exchange	36.9 ppb	NA	46.2 ppb	NA
Free tropospheric contribution to the initial ozone mixing ratio after exchange	7.4 ppb	NA	11.1 ppb	NA
Percent of initial ozone from the free troposphere	17%	NA	19%	NA
After Chemistry				
Final ozone mixing ratio	45.0 ppb	48.9 ppb	57.7 ppb	58.1 ppb
Net ozone production rate (ppb/hour)	0.3	0.2	0.2	0.1

In the base case, the exchange process dilutes the boundary layer ozone and the free tropospheric contribution to the initial boundary layer ozone mixing ratio just after mixing is about 7 ppb or 17% of the initial boundary layer ozone mixing ratio (Table VII). The average subsequent net ozone production rate is about 0.3 ppb/hour, or less than 1 ppb over the two-hour period. For the perturbation case, the exchange process leads to increased boundary layer ozone and the free tropospheric contribution increases to 11 ppb. More importantly, the net ozone production rate is reduced to 0.2 ppb/hour. The net ozone production rate also decreases for periods in the perturbation case with no exchange. So, in general, the net ozone production in the boundary layer decreases when the free tropospheric mixing ratios of ozone are increased. Therefore, the boundary layer ozone response to increasing free tropospheric ozone by 50% over the six-month period must be due to the direct effect of the

exchange process and not the subsequent photochemistry. (Note that this same conclusion is reached when dry deposition is not included in the net ozone production rate.) A comparison of marine and continental sites and month by month comparisons yield conclusions similar to those stated above. It is important to note that the above conclusions do not imply that the photochemical production is not an important source of boundary layer ozone. It simply states that the ***response*** of boundary layer ozone to increased free tropospheric ozone is determined by direct exchange with the free troposphere.

3.5. Average month by month boundary layer ozone responses

Figure 5 and Figure 6 show the absolute and relative boundary layer ozone responses to changing all the free tropospheric mixing ratios by 50% (scenarios 1 and 5), on a monthly basis, averaged over all fifteen grids. The largest absolute response in boundary layer ozone occurs, on average, in May and June when reducing or increasing all free tropospheric mixing ratios by 50% results in absolute changes of around 20 ppb. The largest relative changes occur in April when ozone mixing ratios increase or decrease by 40% when all the free tropospheric mixing ratios are increased or decreased by 50%. Minimum relative responses occur in June and July, while the minimum absolute responses are found in September. Similar results with smaller magnitudes are found for scenario 2 and scenario 6 in which only free tropospheric ozone is changed by 50% (Figure 7 and Figure 8). The boundary layer ozone response to varying the nitrogen and carbon species by 50% (not shown) are fairly uniform across all months with relative changes of 2% to 3% and 6% to 8%, respectively, and absolute changes of about 1 ppb to 2 ppb and 3 ppb to 4 ppb, respectively.

These monthly ozone responses of scenarios 1, 2, 5, and 6 can be explained with three considerations. First, photochemical production of ozone in the boundary layer is expected to be greatest during the summer months, especially June and July when the intensity of solar radiation is at its greatest. Second, model mixing ratios of free tropospheric ozone, the key species in the exchange process, are maximum in May and in June and minimum in September (Figure 2). Finally, the amount of exchange between the free troposphere and the boundary layer as predicted by the EMEP Ozone Model is maximum in April and minimum in June and July (not shown). In April and May, when photochemical activity is still relatively low, large amounts of ozone are mixed into the boundary layer, giving greater importance to the free tropospheric source of boundary layer ozone. In June and July when photochemical activity is maximum, the relative influence of the free troposphere is less dramatic. The September minimum in absolute boundary layer ozone response is easily explained by the fact that free tropospheric ozone mixing ratios are at a minimum during this month.

As discussed in the introduction, Simpson (1992) studies the boundary layer ozone response to several free tropospheric scenarios for July 1985. The responses seen in the present study are much larger than those obtained by Simpson. For example, Simpson finds average relative reductions in boundary layer ozone of about 5% when the free tropospheric ozone is reduced by 20%, while in the present study, the relative reduction for this same scenario is about 10%, when averaged over all fifteen sites. There are several reasons for the difference. Most importantly, the model version used by Simpson does not include cloud venting which is a significant mechanism of exchange (Simpson, 1992). In addition, the time periods (July 1985 versus July 1989) and the subsets of grids used to obtain the above mentioned values are different.

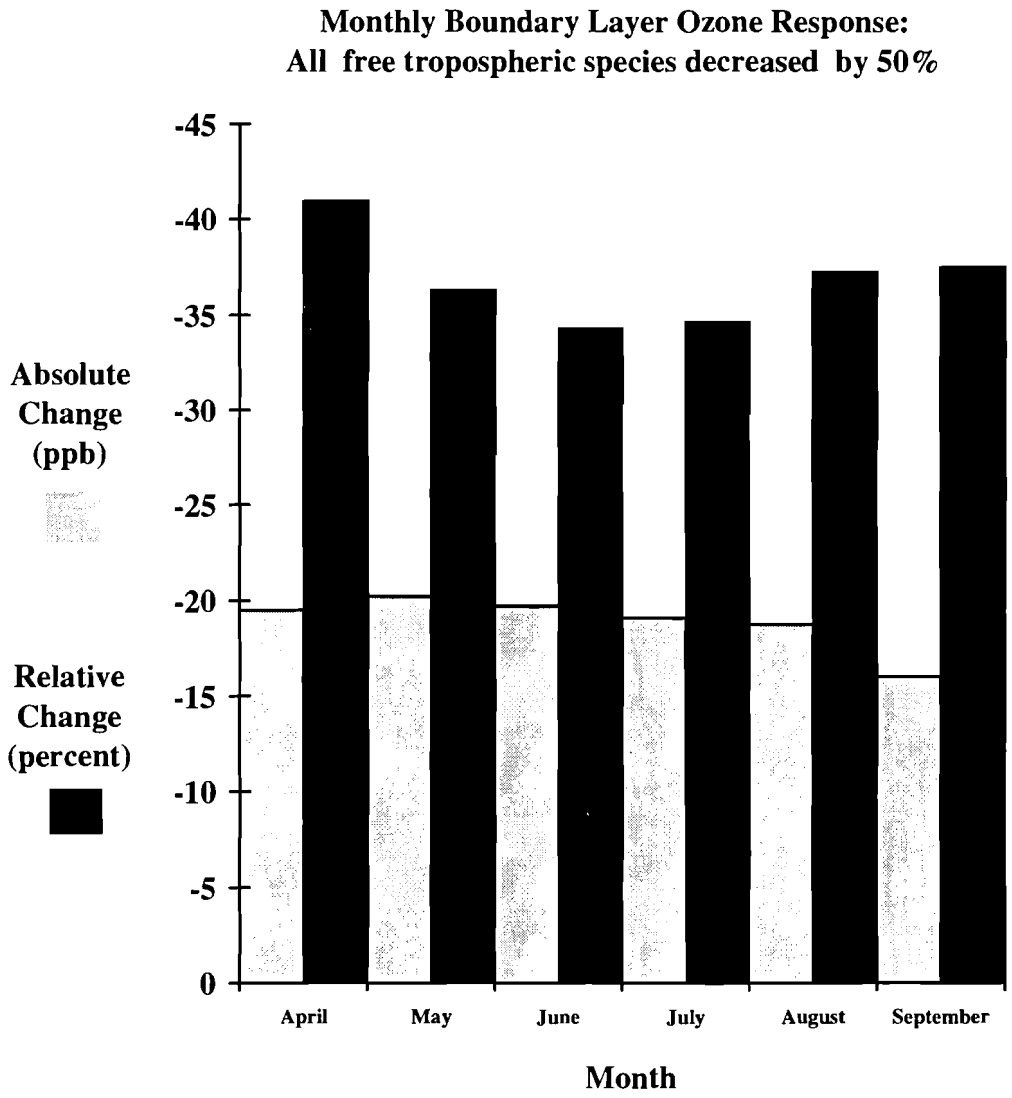

Figure 5. The monthly absolute and relative changes in boundary layer ozone over all fifteen sites for scenario 1 when compared to the base case.

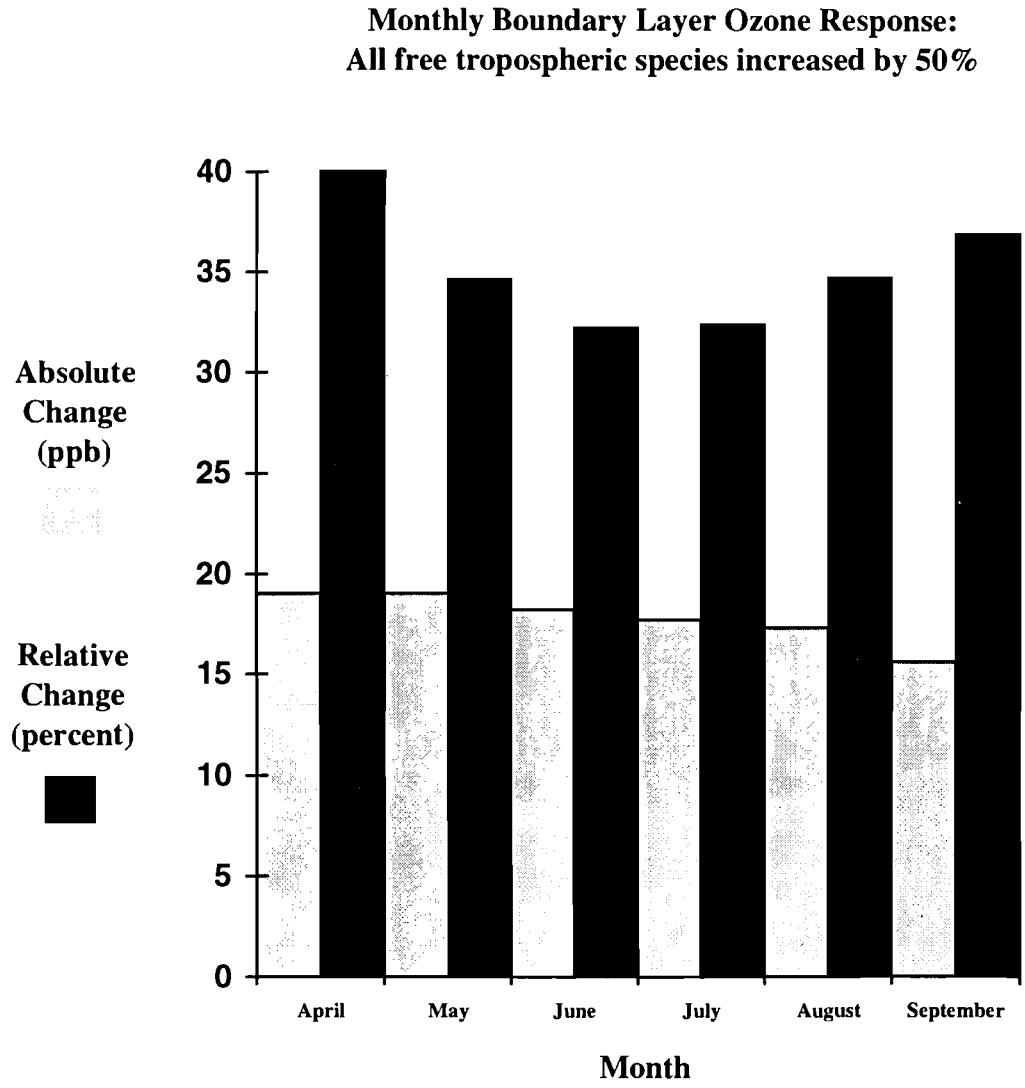

Figure 6. The monthly absolute and relative changes in boundary layer ozone over all fifteen sites for scenario 5 when compared to the base case.

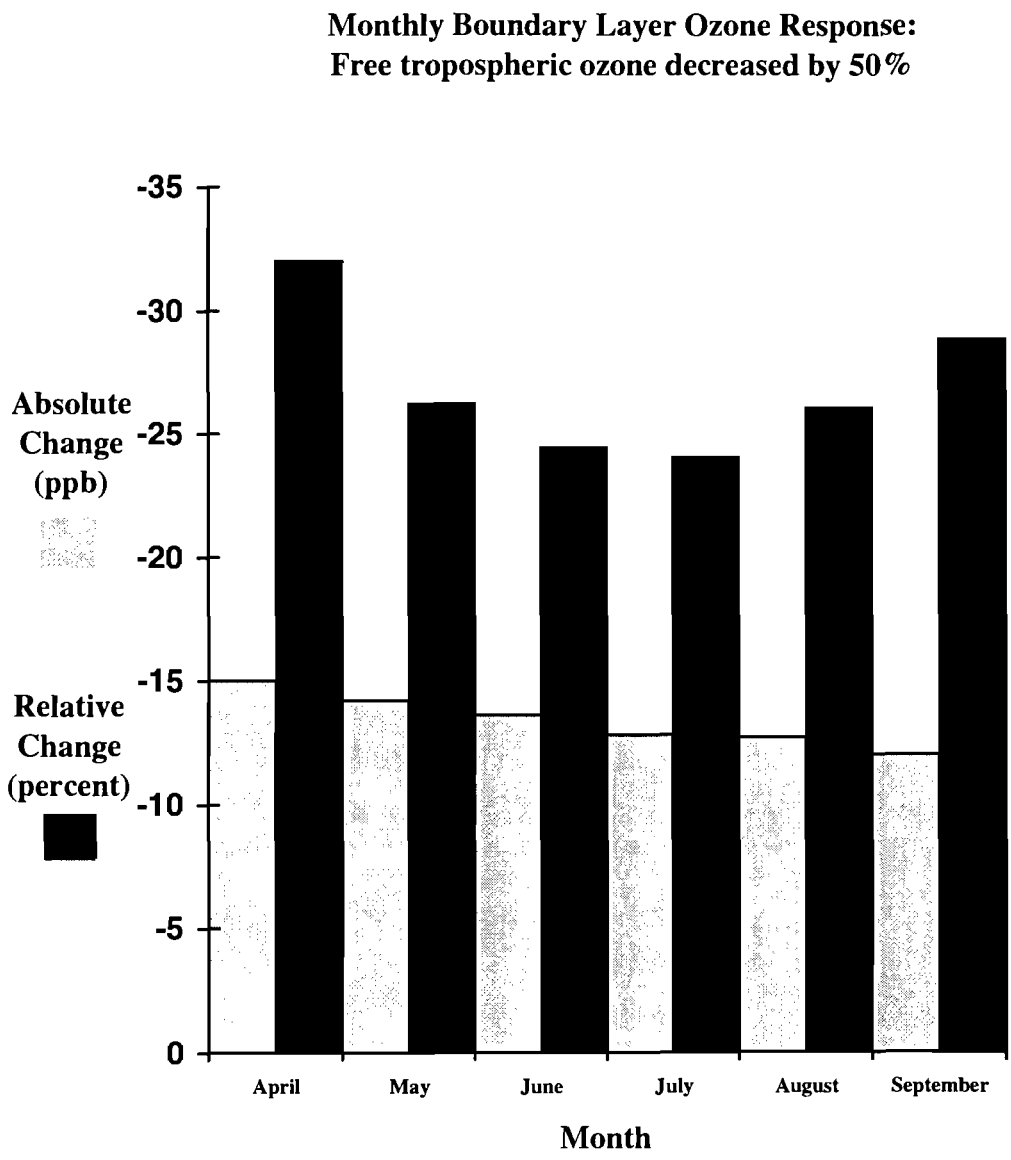

Figure 7. The monthly absolute and relative changes in boundary layer ozone over all fifteen sites for scenario 2 when compared to the base case.

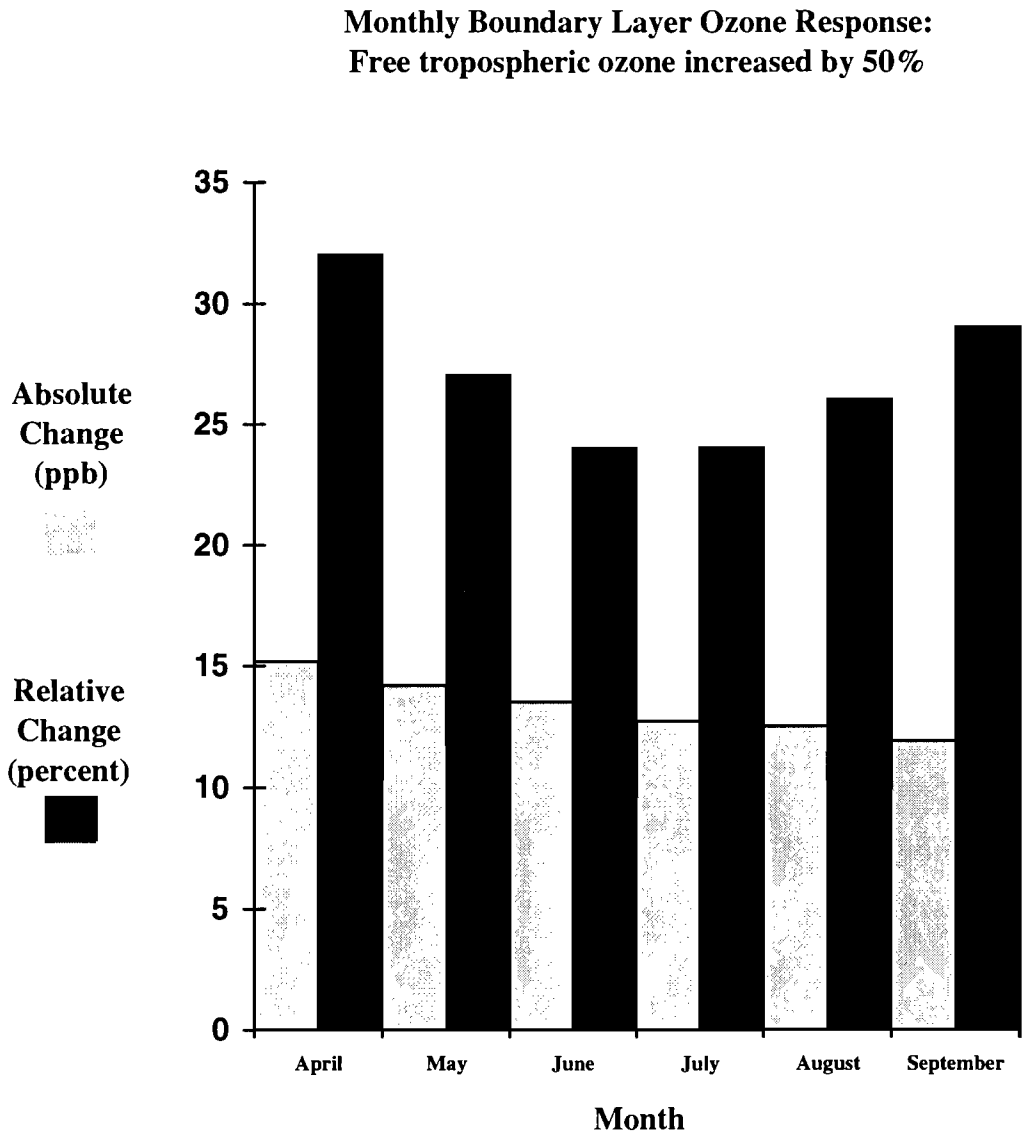

Figure 8. The monthly absolute and relative changes in boundary layer ozone over all fifteen sites for scenario 6 when compared to the base case.

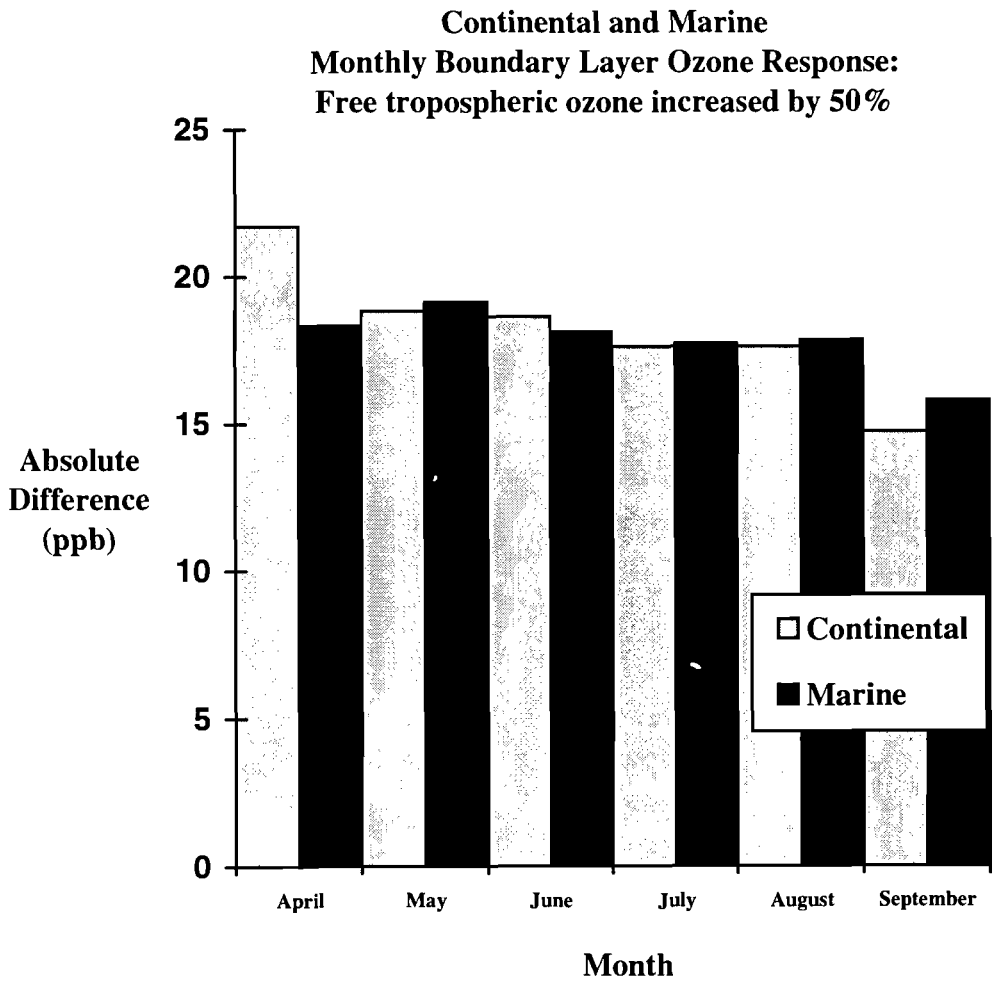

Figure 9. A comparison of absolute monthly ozone responses for continental and marine sites for scenario 6, in which the free tropospheric ozone is increased by 50%, when compared to the base case.

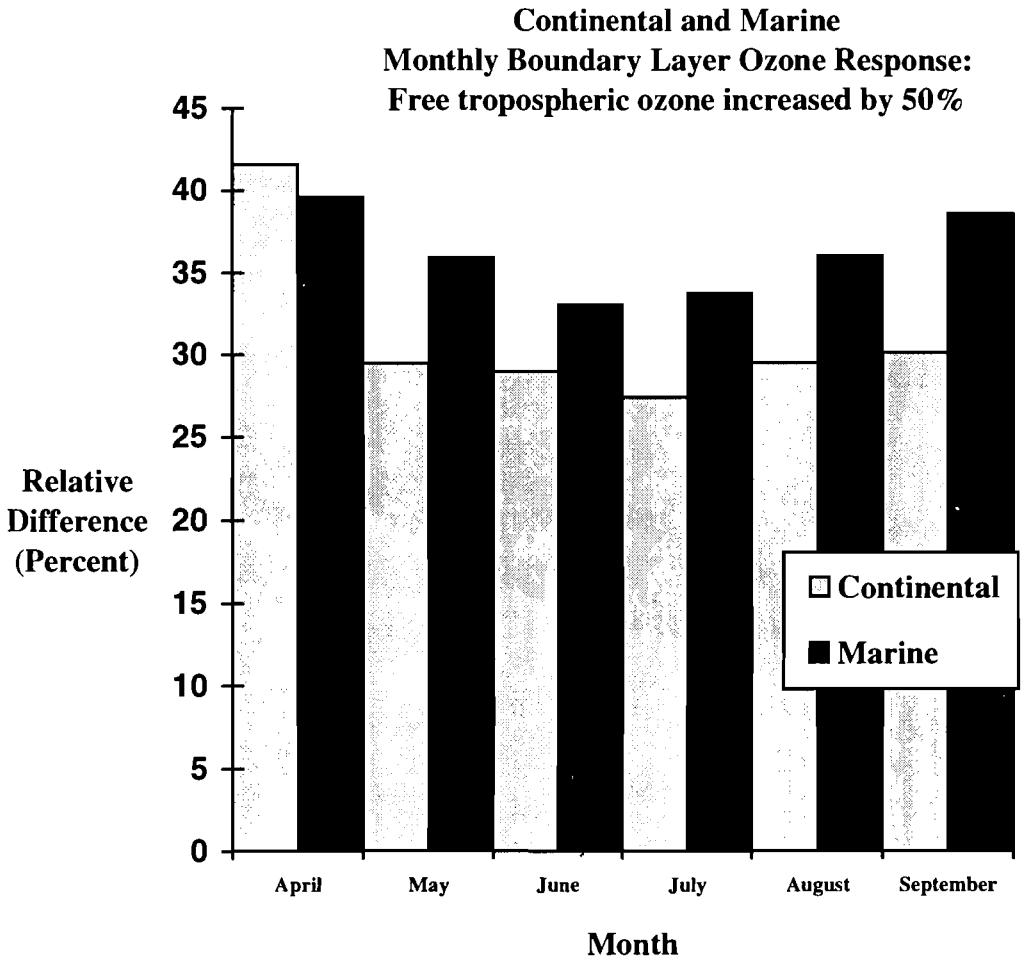

Figure 10. A comparison of relative monthly ozone responses between continental and marine sites for the scenario 6, in which the free tropospheric ozone is increased, by 50% when compared to the base case.

3.6. Continental and marine site boundary layer ozone responses

In this section, the boundary layer ozone responses for marine sites and continental sites are compared. The marine sites are those grids which are likely influenced by air parcels flowing over large water bodies such as the Atlantic Ocean and the Mediterranean Sea, while the continental sites are those which are not located near large water bodies (see Table IV and Figure 3). It is expected that the marine sites will be influenced by less polluted air in comparison to the continental sites. It should be noted that there are twelve marine sites but only three continental sites, and therefore, any conclusions drawn from the following comparisons of these two regimes are preliminary until more continental sites are investigated.

Table VIII presents a comparison of the monthly ozone responses of continental and marine sites for scenario 6 over all sites. While the absolute differences listed in Table VIII are similar between the two regimes, the relative difference is larger for the marine sites, suggesting that the free troposphere plays a larger role in determining boundary layer ozone mixing ratios in areas influenced directly by marine air masses in comparison to areas influenced by continental air masses. Note that the mean ozone mixing ratio for the continental sites over all months is greater than that for the marine sites.

Table VIII. Absolute and relative differences in boundary layer ozone mixing ratios between the base case and scenario 6 in which the free tropospheric ozone is increased by 50%, for marine and continental locations. The base case average ozone mixing ratios for these two regimes are also listed. Standard deviations for the differences are given in parentheses.

Regime	Base Case Ozone (ppb)	Absolute Difference (ppb)	Relative Difference (%)
Marine	53.0	18.7 (4.8)	37.7 (11.2)
Continental	63.1	19.5 (6.2)	33.3 (12.5)

Figure 9 and Figure 10 give a similar comparison between the two regimes but on a month by month basis for scenario 6. The absolute ozone responses shown in Figure 9 suggest that only in April is there a sizable difference between the absolute responses of the two regimes. However, Figure 10 shows that boundary layer ozone at the marine sites is more sensitive to changes in free tropospheric ozone than the continental sites for all months except for April. This finding is consistent with the average data given in Table VIII.

3.7. Daily variability of the boundary layer ozone responses

To show the day to day variability of the boundary layer ozone response, data for seven sites (three continental and four marine) in the form of statistical boxplots are presented in Figure 11 for scenario 6. The data in this figure are the relative changes in boundary layer ozone for each of the 183 12 GMT ozone mixing ratios for each site listed. In general, the relative boundary layer ozone response to a free tropospheric ozone increase of 50% ranges from about 0% to almost 60%. Monthly differences in the amount of free tropospheric

ozone and daily differences in the amount of air exchanged between the free troposphere and the boundary layer explain the wide range of responses.

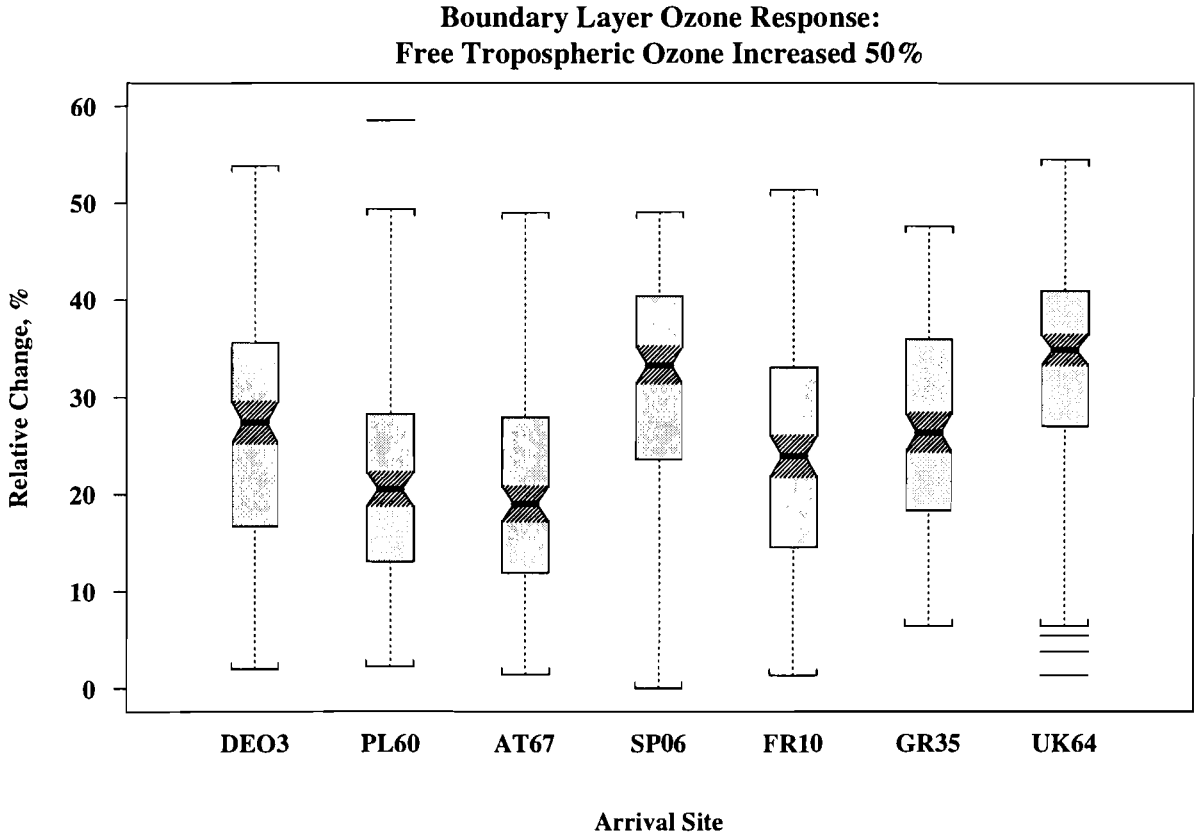

Figure 11. Boxplots for ozone mixing ratios of seven sites (see Table III). Included in each boxplot are the 183 12 GMT ozone mixing ratios spanning the six-month model period.

3.8. Effect of updating the EMEP free tropospheric conditions

Finally, as discussed in section 2.6, the free tropospheric conditions in the EMEP Ozone Model should be updated to reflect recent measurements. Ozone mixing ratios predicted by using the model with the suggested mixing ratios are reduced by about 2% when averaged over all months and all sites in comparison to the base case mixing ratios. In accordance with published measurements, the magnitude of the free tropospheric ozone mixing ratios are not updated in this simulation, but the monthly maximum is shifted. The only species whose magnitudes are changed significantly are some nitrogen species and some carbon species (see section 2.6). As seen above, boundary layer ozone is not very sensitive to changes in the free tropospheric nitrogen and carbon species and so this small response to the updated boundary conditions is not surprising.

4. MODELING SYSTEMS

The results of the sensitivity studies presented in the previous section indicate that free tropospheric species can have a large influence on boundary layer ozone, as predicted by the EMEP Ozone Model. Fortunately, the seasonal model implicitly includes the present influence of the free troposphere as it is formulated in the EMEP model. However, as discussed above, the composition of the free troposphere over Europe is changing, but changes in the composition of the free troposphere cannot be accounted for in the current formulation of the seasonal model.

Such considerations suggest that the free tropospheric source of boundary layer ozone somehow should be included explicitly in the seasonal model as a predictor of boundary layer ozone, along with the predictors for NOx and VOC emissions. In this way, the seasonal model can be used with confidence for future conditions when the composition of the free troposphere may be substantially different from its present composition.

The new seasonal model could be developed strictly from the EMEP Ozone Model which contains a crude parameterization linking European NOx emission changes and free tropospheric ozone changes. However, the source region which determines the composition of the free troposphere over Europe is unknown, although it is possible that Europe, North America, and Asia play a role. Therefore, a more desirable approach of developing the new seasonal model involves implementing the EMEP Ozone Model with free tropospheric mixing ratios produced by models capable of relating emission changes on regional, hemispheric, or global scales to the temporal and spatial composition of the free troposphere over the EMEP domain. The premise underlying the development of the new seasonal model is that the seasonal model should be able to account for changes in the free tropospheric composition and does not imply that the EMEP Ozone Model predictions under present conditions are uncertain.

In this section, various models which may be used to obtain the necessary free tropospheric conditions are reviewed. Models which resolve urban, regional, hemispheric and/or global scales are discussed, and where possible, the performance of these models is examined. The EMEP model accounts for the monthly, latitudinal, and geographic (oceanic versus continental) variations of the free troposphere, as discussed in section 2.6. Therefore, the free tropospheric mixing ratios predicted by other models for use in the EMEP model should predict mixing ratios of ozone, PAN, NOx, VOCs, and other compounds with at least monthly resolution, over a six month period. The spatial resolution does not have to be as fine as the EMEP domain, but should give at least latitudinal and geographical variations. These requirements are emphasized in the following discussion.

4.1. Three-dimensional models

Met O (APR) Model

The MET O (APR) Model is a Lagrangian, three-dimensional, global-scale model of tropospheric chemistry and describes the cycling of 50 species including ozone, CH_4, CO_2, NOx, and nine emitted organics. The chemical mechanism, which has a five-minute time step, considers 100 chemical reactions including 16 photolysis reactions with full diurnal treatment. The emission database of 16 species includes anthropogenic, biomass, vegetation, soil, ocean, aircraft, lightning and stratospheric sources. The meteorological data for this

model is provided by the UK Meteorological Office global model. The model contains a transport mechanism which utilizes a three-hour time step but does not consider subgrid-scale convection or synoptic-scale convection. The horizontal resolution of the output is 10° by 10° while the vertical resolution is variable with about 1 km thick layers below 700 hPa but larger thicknesses up to the model top of 16 km (Collins et al., 1995). The Met O (APR) Model can provide the needed spatial and temporal resolution of all free tropospheric species necessary for the EMEP Ozone Model.

The Met O (APR) Model output has been compared against observational and other studies. Model predictions of global average OH mixing ratios are in reasonable agreement with previous results. The model overpredicts NOy mixing ratios in northern Canada, but produces mixing ratios in general agreement with observations from the eastern United States. Northern and southern hemispheric surface oceanic ozone mixing ratios are in agreement with observations except that northern hemispheric predictions of ozone show a plume (>40 ppb) at the surface of the Atlantic Ocean between 30°N and 40°N which is not found in observations. In remote areas, the model overestimates the observed summer minima in ozone at the ocean surface and underestimates winter mixing ratios. The geographical distribution of summer daily maximum ozone predictions over Europe is similar to that predicted by the EMEP Ozone Model (Simpson, 1993), but the magnitudes are overpredicted by between 10 ppb and 20 ppb. In general, the model results agree with observations where surface emissions do not vary significantly over a 10° by 10° area (Collins et al., 1995).

MOGUNTIA

The Model Of the General UNiversal Tracer transport In the Atmosphere (MOGUNTIA) has been developed at the Max-Planck-Institute for Chemistry and is designed to numerically simulate the global tropospheric transport of species (Zimmerman, et al., 1989). The horizontal grid size of MOGUNTIA is 10° by 10° with vertical grids up to 100 hPa. The meteorological inputs to the model are monthly mean values of temperature and winds, and with these, the model computes vertical velocities, turbulent diffusion, and mixed layer heights (e.g., Zimmerman, 1987). Outputs include monthly average mixing ratios which vary according to latitude, longitude, and altitude over the globe. A chemical mechanism describing the O_3-H_2O-CH_4-CO-NOx system which also includes heterogeneous reactions of NO_3 and N_2O_5 on sulfate aerosols has been implemented into MOGUNTIA (Dentener and Crutzen, 1993; Crutzen and Zimmerman, 1991). With these chemical schemes, MOGUNTIA can output the monthly data over Europe required for use in the EMEP Ozone Model.

MOGUNTIA has been shown to reproduce the main features of annual meridional distributions of OH radicals and can simulate the observed growth in ozone and CO that occurred from pre-industrial times until 1980 (Crutzen and Zimmerman, 1991). The spatial ozone distribution predicted by this model contains features found in observations such as higher ozone mixing ratios downwind of industrial regions. However, it cannot simulate episodes of high ozone mixing ratios in the summer and underestimates ozone in the middle and upper troposphere at mid-latitudes (Crutzen and Zimmerman, 1991).

IMAGES

The Intermediate Model of Global Evolution of Species (IMAGES) is designed to study the global distribution, budgets, and trends of various tropospheric compounds. The

"intermediate" aspect of this model stems from the transport scheme which is intermediate between highly parameterized one-dimensional models and fully explicit coupled GCM and tracer models. Developed to be integrated with long time-steps while still considering diurnal variations of solar radiation, IMAGES requires a factor of 10 less computer resources than three-dimensional chemistry models coupled to GCMs. Along with dry and wet deposition, the model contains a chemical scheme which considers 125 chemical reactions, 26 photodissociations, and some heterogeneous reactions on aerosols. Monthly mean climatological winds which drive the advection are from the European Center for Medium-Range Weather Forecasts (ECMWF) analysis, as are all other meteorological inputs. Convection by cumulonimbus clouds is considered as well. The domain of the model is divided into 5° by 5° grids, over 25 vertical layers from the surface to 50 hPa. The output of IMAGES consists of monthly mixing ratios of 41 species including ozone, nitrogen compounds (NOx, HNO_3), CO, and hydrocarbons (CH_4, C_2H_6, C_3H_6) over the globe (Müller and Brasseur, 1995). Therefore, the output of IMAGES is ideal for use in the EMEP Model.

The output of IMAGES has been compared to observations. The methane mixing ratio predictions agree well with observations site by site and in terms of the interhemispheric difference. CO predictions are found to be comparable to observations in the southern hemisphere and in the tropics but are too low in the northern hemisphere. Comparisons involving NO also produce mixed results, as IMAGES underpredicts upper tropospheric NO but computes reasonable values for the Amazon region. IMAGES reproduces the high mixing ratios of ozone downwind of sources, but overpredicts wintertime surface ozone at northern mid-latitudes. Vertical profiles of ozone predicted by the model are also in good agreement with observations (Müller and Brasseur, 1995).

Other three-dimensional modeling systems

While the Met O (APR), MOGUNTIA, and IMAGES systems are currently operational in terms of the data requirements of the EMEP model, several other existing modeling systems would require alterations or further developments before they could be used with the EMEP Model. Some of these models are discussed below.

EURAD

The European Acid Deposition Model (EURAD) simulates the transport, chemical transformation, and deposition of trace tropospheric constituents over Europe. The modeling system contains three major components: 1.) EURAD emissions model, 2.) meteorological fields given by the Penn State/NCAR mesoscale model MM4 or MM5, and 3.) the Chemistry Transport Module (CTM), which is driven by numbers 1.) and 2.). The domain of EURAD is most of Europe and part of the North Atlantic and has a horizontal resolution of 63.5 km over 15 vertical layers. The model predicts three-dimensional mixing ratios of 39 species and wet and dry deposition of some of these species as influenced by advection, diffusion, chemical transformation, and cloud processes (Hass et al., 1993). The RADM2 chemical mechanism as developed by Stockwell et al. (1990) is used in EURAD and the PHOXA and EMEP emission databases have been implemented in this system (Hass et al., 1993; Jakobs, 1994). EURAD has been shown to adequately predict surface mixing ratios of SO_2 and NO_2, but underpredicts sulfate mixing ratios (Hass et al., 1993). Because this model is designed to study periods of a few days and because the domain is smaller than that of the EMEP model, the EURAD system would need considerable alterations before its output could be used with the EMEP model.

TADAP

The Transport and Deposition of Acidifying Pollutants (TADAP) model is a comprehensive, three-dimensional model designed for the simulation of the coupled photochemical oxidant/acid deposition system over Europe. It is based on the Acid Deposition and Oxidant Model (ADOM), developed for similar purposes over North America. The horizontal resolution of TADAP is about 100 km, while the vertical dimension contains 12 unevenly spaced levels between 0 km and 10 km. The model includes modules for transport and wet and dry removal. The chemical reaction sequence consists of 100 reactions among 50 species, 30 of which are transported species. Emission inputs to the model include NOx, SOx, and reactive hydrocarbons. This model is designed to study episodic events of a few days (Venkatram and Karamchandani, 1988). Like the EURAD system, the temporal scale of TADAP would need to be extended if it were to be used in conjunction with the EMEP model.

GETTM/RADM/SAQM

A fully-nested, three-dimensional modeling system in which interactions between the urban, regional, and global environments are explicitly considered is currently being developed by the Atmospheric Modeling Section at the Atmospheric Sciences Research Center of the State University of New York at Albany (SUNY-Albany), Albany, NY, USA. The system is designed to study the interactions among meteorological, chemical, and physical processes which determine the long-range transport, transformation, and removal of short-lived atmospheric species on time scales of a few days to two months.

When this modeling system is fully operational, the small-scale models can provide high resolution to the larger-scale models and larger-scale models can provide time-dependent boundary conditions to the smaller-scale models. In this way, the interactions between urban or regional scales and the global environment can be studied effectively (Chang et al., 1987; Li, 1995; Jin and Chang, 1995).

GFDL GCTM

The Global Chemical Transport Model (GCTM) developed at the Geophysical Fluid Dynamics Laboratory (GFDL) is an 11-level global model with a horizontal resolution of about 265 km. The meteorological data for the model, provided by a parent global circulation model (GCM) (Manabe et al., 1974; Manabe and Holloway, 1975), includes 12 months of 6-hour, time-averaged wind and total precipitation fields. The GCTM considers horizontal sub-grid scale transport, vertical mixing by dry and moist convection, dry deposition based on measured deposition velocities of individual reactive nitrogen species, and a wet removal scheme which considers shallow-convective or deep-convective precipitation (Levy and Moxim, 1989; Manabe and Holloway, 1975).

A recent study by Kasibhatla et al. (1993) uses the GFDL GCTM to examine the global distributions of NOx, PAN, HNO_3, and NOy by using the output of an off-line O_3-CO-CH_4-NOx-HxOy chemical scheme as two-dimensional input to the three-dimensional model. Inputs to this off-line chemical scheme include hemispherically-averaged one-dimensional CO and NOx profiles. The global three-dimensional model includes detailed emission inventories from the United States, Canada, and Europe. While the GCTM is currently operational, it can provide only the three-dimensional nitrogen species mixing ratios and

therefore, would require a more advanced chemical scheme if it is to be provide free tropospheric data to the EMEP Model.

GISS GCM

Jacob et al. (1993a,b) use the Goddard Institute for Space Studies General Circulation Model (GISS GCM) (Hansen et al., 1983) as the meteorological driver model for a study of ozone over North America, Central America, and surrounding water bodies. Similarly, Balkanski et al. (1993) used the GISS GCM to study the global distribution of Lead-210. To use the GISS GCM to study ozone and its precursors in the lower free troposphere of Europe, the domain would have to be modified and a detailed chemical scheme such as that used by Jacob et al. would have to be implemented.

GLOMAC1

A global, three-dimensional, tracer transport model (GLOMAC1) was developed to study feedback mechanisms between climate and atmospheric chemistry. GLOMAC1 is based on a GCM known as ECHAM2 which is a low-resolution version of the European Center for Medium Range Weather Forecasting (ECMWF) model. ECHAM2 has a hybrid coordinate system with 19 vertical layers and a horizontal resolution of 5.625° latitude and longitude. In the ECHAM2/GLOMAC1 system, the tracer transport scheme is contained inside the meteorological model and calculates the effects of emission, advection, diffusion, wet and dry removal, and chemical transformations of the chemical constituents. Recent studies of the global transport of Lead-210 (Feichter et al., 1991) and Beryllium-7 (Brost et al., 1991) as tracer species suggests that the model transport and wet deposition components are reasonable. To output the data necessary for the EMEP Model, a detailed chemical mechanism would have to be implemented into this model.

4.2. Two-dimensional models

The two-dimensional models discussed below are all latitude-height models. In other words, there is no variation in east-west direction. Because the EMEP domain contains east-west oceanic and continental regimes which may have very different chemical compositions, the output from these models is not ideal for providing the required detail for the EMEP free tropospheric mixing ratios. However, these models are computationally much more efficient than the more complex three-dimensional models and they may be of use in studying the average influence of emission changes on the free troposphere. The output from these models might be used to guide the selection of free tropospheric boundary conditions for the EMEP model.

Cambridge Model

The Cambridge model (Harwood and Pyle, 1975 and 1977) is a two-dimensional global model with a horizontal resolution of 9.47° and a vertical resolution of about 3.5 km up to 60 km. It is an Eulerian model for which averaging takes place over longitude at a fixed latitude, altitude, and time. Mean circulation in the Cambridge model is calculated based on forcing by latent and radiative heating and eddy transport processes. Because the model does not contain treatment of a boundary layer and its resolution in the troposphere is quite coarse, this model is best considered a model of the free troposphere (Law and Pyle, 1993). The chemical scheme in the model is a family approach in which a photochemical steady state is assumed for the species with short chemical lifetimes compared to their dynamical lifetimes. In this sense, the distribution of these species is determined by chemical processes rather than

dynamical processes. The families or groups of species such as Ox, NOx, HOx are then transported as a whole. Emissions of species are specified latitudinally and monthly. Removal processes in the model include both wet and dry deposition (Law and Pyle, 1991 and 1993).

When compared to observations, the Cambridge model is found to produce mixing ratios of nitrogen species which are comparable to observations at northern hemisphere polluted sites. In the southern hemisphere, however, the model predictions are comparable to remote observations. Ozone predictions in the northern hemisphere are higher than those values observed at remote locations and the seasonal pattern matches observations at more polluted sites with summer maxima at the surface (Law and Pyle, 1993). The methane mixing ratios predicted by the Cambridge model show observed features, although northern hemispheric mixing ratios are overpredicted. Finally, comparison of CO predictions with observations shows the model overpredicts mixing ratios at clean air sites and underpredicts those at polluted sites.

Isaksen/Rodhe Model

This model is a two-dimensional model with a horizontal resolution of 10° and a vertical resolution of 250 m up to 3.25 km and 1 km from here up to 17 km. The domain stretches from 85° N to 85° S latitude. The distribution of tropospheric trace species such as O_3, PAN, and CO is predicted by chemical reactions, precipitation, dry deposition of particulate matter, and by emissions of hydrocarbons and nitrogen oxides from natural and anthropogenic sources (Isaksen and Hov, 1987; Rodhe and Isaksen, 1980; Isaksen and Rodhe, 1978). CO mixing ratios predicted by this model reproduce observed latitudinal variations, but middle tropospheric values are about 30% underpredicted. In contrast, free tropospheric ozone is overpredicted by this model, although the mid-latitude, northern hemisphere maximum in ozone is reproduced. Finally, OH mixing ratios at the surface are found to be in agreement with observations over Europe (Isaksen and Hov, 1987).

Strand/ Hov Model

The model developed by Strand and Hov (1994) is a two-dimensional model designed to study tropospheric ozone production. The transport of chemical species in this model is determined by the transport model of Strand and Hov (1993), which uses a horizontal resolution of 75 equally spaced latitude points from pole to pole and a vertical resolution of 33 equally-spaced pressure levels from 1000 hPa to 10 hPa. The chemical mechanism in the model involves 126 chemical reactions and 44 chemical species and is similar to the one currently used in the EMEP Ozone Model. Emissions include natural and anthropogenic nitrogen oxides, carbon monoxide, and the most important hydrocarbons for a total of 11 emitted species. Stratospheric sources are also considered. The removal processes include dry and wet deposition. The model reproduces well the observed annual variation of ozone in the meridional plane. In addition, the model predictions of other chemical species such as nitrogen oxides, CO, and hydrocarbons also agree with observations to within expectations of a two-dimensional model (Strand and Hov, 1994).

Hough/Johnson Model

This two-dimensional model consists of a grid extending from pole to pole and from the surface up to 24 km. Monthly atmospheric circulations and temperature fields drive the meteorological portion of the model. The emission inventory contains 17 species including N_2O, NO, CO, H_2, CH_4, and 12 non-methane hydrocarbons. The chemical mechanism

includes 56 chemical species which are involved in 90 thermal reactions and 27 photolytic processes. The model also includes nighttime NOy chemistry, dry deposition, and wet deposition (Hough, 1989; Hough and Johnson, 1991). The annual surface ozone variations produced by this model agree with observations from Europe, Somoa, and the South Pole. However, the model overpredicts middle tropospheric ozone values at middle and high latitudes of the northern hemisphere. PAN predictions are consistent with observations except over the northern high latitudes where the model overpredicts PAN mixing ratios (Hough and Johnson, 1991).

5. CONCLUSIONS

The seasonal model, which is based on the output of the EMEP ozone model, is an important part of the integrated assessment model for surface ozone over Europe. In its present form, it considers only emissions of NOx and VOCs to predict boundary layer ozone mixing ratios. Sensitivity studies performed here involving the free tropospheric conditions in the EMEP model, however, suggest that the free tropospheric source of boundary layer ozone also should be explicitly accounted for in the seasonal model. Free tropospheric ozone is found to be the most important species in this exchange process, while grouped nitrogen and carbon compounds have a lesser influence. The response of boundary layer ozone to increasing free tropospheric ozone by 50% is found to be due to the direct mixing of ozone into the boundary layer and not chemical changes in the boundary layer caused by injections of increased ozone. In general, the absolute boundary layer ozone response is 50% of the free tropospheric perturbation. On a monthly basis, boundary layer ozone is most sensitive to free tropospheric changes in April because of large free tropospheric ozone mixing ratios and because of large air exchange between the free troposphere and the boundary layer during this month. Ozone mixing ratios at sites with a marine influence are found to be more sensitive to changes in the free troposphere than those at continental locations in relative terms; the absolute sensitivities for these two regimes are comparable. It should be remembered that these conclusions are based only on the conditions of April through September, 1989.

When developing an updated version of the seasonal model which includes the influence of the free troposphere, it is important to consider the relationship between emission changes and free tropospheric mixing ratio changes. Such a feedback must be accounted for in the seasonal model since implementation of the seasonal model involves directly changing emissions of NOx and VOCs over Europe. Thus, the relationship between emission changes, free tropospheric composition, and the resulting influence on boundary layer ozone must be determined within the context of the EMEP Ozone Model, upon which the new version of the seasonal model will be developed. This complex relationship may be best handled by computing free tropospheric mixing ratios over Europe for a number of emission scenarios with a tropospheric chemistry/transport model. The computed free tropospheric mixing ratios may then be used in the EMEP model for a study of the influence of the free troposphere on boundary layer ozone which is then consistent with specified emission changes. From these EMEP model runs, the predictor of the free tropospheric influence on boundary layer ozone can be determined. Several modeling systems including the Met O (APR) model, MOGUNTIA, and IMAGES are thought to be candidates for providing the necessary free tropospheric mixing ratios to the EMEP model.

Finally, when considering the relationship between the free troposphere and emission changes over Europe, it is important to recognize that emissions from regions other than Europe may affect the European troposphere. For example, Jacob et al. (1993b) conclude that 70% of the net ozone production in the United States boundary layer is exported, with most of it being vented into the free troposphere where it contributes substantially to hemispheric ozone levels. Similar conclusions are reached by Parrish et al. (1993). These findings, in conjunction with the current finding of the importance of free tropospheric ozone to boundary layer ozone over Europe, emphasize the need to consider regional, hemispheric, and global scales in the study of the link between emission control strategies, the free troposphere, and boundary layer ozone over Europe.

REFERENCES

Allam, R. J., and A. F. Tuck, Transport of water vapour in a stratosphere-troposphere general circulation model. 2. trajectories, *Quart. J. Roy. Meteorol. Soc.*, **110**, 357-392, 1984.

Altshuller, A. P., Review: natural volatile organic substances and their effect on air quality in the United States, *Atmos. Environ.*, **17**, 2131-2165, 1983.

Bakwin, P. S., P. P. Tans, and P. C. Novelli, Carbon monoxide budget in the Northern Hemisphere, *Geophys. Res. Lett.*, **21**, 433-436, 1994.

Balkanski, Y. L., D. J. Jacob, and G. M. Gardner, Transport and residence times of aerosols inferred from a global three-dimensional simulation of ^{210}Pb, *J. Geophys. Res.*, **98**, 20,573-20,586, 1993.

Bamber, D. J., P. G. Healey, B. M. Jones, S. A. Penkett, A. F. Tuck, and G. Vaughn, Vertical profiles of tropospheric gases--chemical consequences of stratospheric intrusions, *Atmos. Environ.*, **18**, 1759-1766, 1984.

Baykal, A., S. G. Tuncel, U. Özer, Measurement of gas phase pollutants at Uludag Mountain of northwest Turkey, In: *Proc. EUROTRAC Symposium '94*, ed. P. M. Borrell, P. Borrell, T. Cvitas, and W. Seiler, Garmisch-Partenkirchen, F. R. G., 11-15 April, 1994.

Beekman, M., G. Ancellet, and G. Megie, Climatology of tropospheric ozone in southern Europe and its relation to potential vorticity. *J. Geophys. Res.*, **99**, 12,841-12,853, 1994.

Bekki, S., K. S. Law, and J. A. Pyle, Effect of ozone depletion on atmospheric CH_4 and CO concentrations, *Nature*, **371**, 595-597, 1994.

Bojkov, R. D. Ozone changes at the surface and in the free troposphere, in Tropospheric Ozone: Regional and Global Scale Interactions, edited by Ivar S. Isaksen, D. Reidel Publishing Company, Dodrecht, Holland, 1988.

Brost, R. A., J. Feichter, M. Heimann, Three dimensional simulation of ^{7}Be in a global climate model, *J. Geophys. Res.*, **96**, 22,423-22,445, 1991.

Chang, J. S., R. A. Brost, I. S. A. Isaksen, S. Madronich, P. Middleton, W. R. Stockwell, and C. J. Walcek, A three-dimensional Eulerian acid deposition model: physical concepts and formulation, *J. Geophys., Res.*, **92**, 14,681-14,700, 1987.

Collins, W. J., D. S. Stevenson, C. E. Johnson, and R. G. Derwent, Tropospheric ozone modelled with a global-scale Lagrangian model of diurnal atmospheric chemistry, *Met O (APR) Turbulence and Diffusion Note No. 224*, UK Meteorological Office, 1995.

Cox, R. A., Atmospheric chemistry of NO_x and hydrocarbons influencing tropospheric ozone, in Tropospheric Ozone: Regional and Global Scale Interactions, edited by Ivar S. Isaksen, D. Reidel Publishing Company, Dodrecht, Holland, 1988.

Crutzen, P. J. and P. H. Zimmerman, The changing photochemistry of the troposphere, *Tellus*, **43AB**, 136-151, 1991.

Davies. T. D., P. M. Kelly, P. S. Low, and C. E. Pierce, Surface ozone concentrations in Europe: links with the regional-scale atmospheric circulation, *J. Geophys. Res.*, **97**, 9819-9832, 1992.

Dentener, F. J. and P. J. Crutzen, Reaction of N_2O_5 on tropospheric aerosols: impact on the global distribution of NOx, O_3, and OH, *J. Geophys. Res.*, **98**, 7149-7163, 1993.

Dlugokencky, E. J., L. P. Steele, P. M. Lang, and K. A. Massarie, The growth rate and distribution of atmospheric methane, *J. Geophys. Res.*, **99**, 17,021-17,043, 1994.

Drummond, J. W., D. H. Ehhalt, and A. Volz, Measurements of nitric oxide between 0-12 km altitude and 67° N to 60° S latitude obtained during STRATOZ III, *J. Geophys. Res.*, **93**, 15,831-15,849, 1988.

Duce, R. A., Mohnen, V. A., Zimmerman, P. R., Grosjean D., Cautreels, W., Chatfield, R., Jaenicke, R., Ogren J. A., Pellizzari, E. D., and G. T. Wallace, Organic material in the global troposphere, *Rev. Geophys. Space Phys.*, **21**, 921-952, 1983.

Ehhalt, D. H., J. Rudolph, F. Meixner, and U. Schmidt, Measurements of selected C2-C5 hydrocarbons in the background troposphere: vertical and latitudinal variations, *J. Atmos. Chem.*, **3**, 29-52, 1985.

Fehsenfeld, F. C., D. D. Parrish, and D. W. Fahey, The measurement of NOx in the non-urban troposphere. in Tropospheric Ozone: Regional and Global Scale Interactions, edited by Ivar S. Isaksen, D. Reidel, Dordrecht, Holland, 1988.

Feichter, J., R. A. Brost, and M. Heimann, Three-dimensional modeling of the concentrations and deposition of ^{210}Pb aerosols, *J. Geophys. Res.*, **96**, 22,447-22,460, 1991.

Field, R. A., M. E. Goldstone, J. N. Lester, and R. Perry, The sources and behaviour of tropospheric anthropogenic volatile hydrocarbons, *Atmos. Environ.*, **16**, 2983-2996, 1992.

Follows, M. J. and J. F. Austin, A zonal average model of the stratospheric contributions to the tropospheric ozone budget, *J. Geophys. Res.*, **97**, 18,047-18,060, 1992.

Greenberg, J. P. and P. R. Zimmerman, Nonmethane hydrocarbons in remote tropical, continental, and marine atmospheres, *J. Geophys. Res.*, **89**, 4767-4778, 1984.

Hansen, J., G. Russle, D. Rind, P. Stone, A. Lacis, S. Lebedeff, R. Reudy, and L. Travis, Efficient three-dimensional global models for climate studies: models I and II, *Mon. Weather Rev.*, **111**, 609-662, 1983.

Harwood, R. S., and J. A. Pyle, A two-dimensional mean circulation model for the atmosphere below 80 km, *Q. J. Roy. Meteorol. Soc.*, **106**, 723-747, 1975.

Harwood, R. S., and J. A. Pyle, Studies of the ozone budget using a mean circulation model and linearized photochemistry, *Q. J. Roy. Meteorol. Soc.*, **101**, 319-343, 1977.

Hass, H., A. Ebel., H. Feldmann, H. J. Jakobs, and M. Memmesheimer, Evaluation studies with a regional chemical transport model (EURAD) using air quality data from the EMEP monitoring network, *Atmos. Environ.*, **27A**, 867-887, 1993.

Heyes, C., W. Schöpp, M. Amann, and S. Unger, A simplified model to predict long-term ozone concentrations in Europe. WP-96-12. International Institute for Applied Systems Analysis (IIASA), Laxenburg, Austria, 1996.

Hoskins, B. J., M. E. McIntyre, and A. W. Robertson, On the use and significance of isentropic potential vorticity maps, *Quart. J. Roy. Meteorol. Soc.*, **111**, 887-946, 1985.

Hough, A. M., The development of a two-dimensional global tropospheric model-- 1. the model transport, *Atmos. Environ.*, **23**, 1235-1261, 1989.

Hough, A. M. and C. E. Johnson, Modeling the role of nitrogen oxides, hydrocarbons and carbon monoxide in the global formation of tropospheric oxidants, *Atmos. Environ.*, **25A**, 1819-1835, 1991.

Hov, O., N. Schimdbauer, and M. Oehme, Light hydrocarbons in the Norwegian Arctic, *Atmos. Environ.*, **23**, 2471-2482, 1989.

Isaksen, I. S. A. and H. A. Rodhe, A two-dimensional model for the global distribution of gases and aerosol particles in the troposphere, *Rep. AC-47*, Dep. of Meteorol., Stockholm, 1978.

Isaksen, I. S. A. and O. Hov, Calculations of the trends in the tropospheric concentrations of O_3, OH, CO, CH_4, and NOx, *Tellus*, **39B**, 271-285, 1987.

Jacob, D. J., J. A. Logan, and R. M. Yevich, Simulations of summertime ozone over North America, *J. Geophys. Res.*, **98**, 14,797-14,815, 1993a.

Jacob, D. J., J. A. Logan, G. M. Gardner, R. M. Yevich, C. M. Spivakovsky, and S. C. Wofsy, Factors regulating ozone over the United States and its export to the global atmosphere, *J. Geophys. Res.*, **98**, 14,817-14,826, 1993b.

Jakobs, H. J., Use of nested models for air pollution studies, In: *Proc. EUROTRAC Symposium '94*, ed. P. M. Borrell, P. Borrell, T. Cvitas, and W. Seiler, Garmisch-Partenkirchen, F. R. G., 11-15 April, 1994.

Jin, S. and J. S. Chang, A three-dimensional non-hydrostatic regional scale SARMAP air quality model (SAQM), submitted to *J. Geophys. Res.*, 1995.

Kanakidou, M. B. Bonsang, and G. Lambert, Light hydrocarbons vertical profiles and fluxes in a French rural area, *Atmos. Environ.*, **23**, 921-927, 1989.

Kasibhatla, P. S., H. Levy, II, and W. J. Moxim, Global NOx, HNO_3, PAN, and NOy distribution from fossil fuel combustion emissions: a model study, *J. Geophys. Res.*, **98**, 7165-7180, 1993.

Khalil, M. A. K. and R. A. Rasmussen, Carbon monoxide in the Earth's atmosphere: indications of a global increase. *Nature*, **332**, 242-245, 1988.

Khalil, M. A. K. and R. A. Rasmussen, Global decrease in atmospheric carbon monoxide concentration, *Nature*, **370**, 639-641, 1994.

Kley, D. , H. Geiss, and V. A. Mohnen, Tropospheric ozone at elevated sites and precursor emissions in the United States and Europe. *Atmos. Environ.* **28**, 149-158, 1994.

Law, K. S. and J. A. Pyle, Modeling trace gas budgets in the troposphere 1. ozone and odd nitrogen, *J. Geophys. Res.*, **98**, 18,377-18,400, 1993.

Law, K. S. and J. A. Pyle, Modelling the response of tropospheric trace species to changing source gas concentrations, Atmos. Environ., **25A**, 1863-1871, 1991.

Levy, H., II and Moxim, W. J., Simulated global distribution and deposition of reactive nitrogen emitted by fossil-fuel combustion, *Tellus*, **41B**, 256-271, 1989.

Li, Y., A three-dimensional global tracer transport model formulated on episodic consideration, Ph.D. thesis, Department of Atmospheric Sciences/Atmospheric Science Research Center, State University of New York at Albany, NY, 1995.

Lightman, P., A. S. Kallend, A. R. W. Marsh, B. M. R. Jones, and S. A. Penkett, Seasonal variation of hydrocarbon in the free troposphere at mid-latitudes, Tellus **42B**, 408-422, 1990.

Liu, S. C. and R. Cicerone, Fixed nitrogen cycle, in Global Tropospheric Chemistry, a Plan for Action, National Academy Press, Washington, D. C., 113-116, 1984.

Liu, S. C., M. Trainer, F. C. Fehsenfeld, D. D. Parrish, E. Williams, D. W. Fahey, G. Hubler, and P. C. Murphy, Ozone production in the rural troposphere and the implications for regional and global ozone distributions. *J. Geophys. Res.*, **92**, 4191-4207, 1987.

Logan, J. A., M. J. Prather, S. C. Wofsy, and M. B. McElroy, Tropospheric chemistry: a global perspective, *J. Geophys. Res.*, **86**, 7210-7254, 1981.

Logan, J. A., Nitrogen oxides in the troposphere: global and regional budgets, *J. Geophys. Res.*, **88**, 10,785-10,807, 1983.

Logan, J. A., Tropospheric ozone: seasonal behavior, trends, and anthropogenic influence, *J. Geophys. Res.*, **90**, 10,463-10,482, 1985.

Manabe, S., D.G. Hahn, and J. L. Holloway, Jr., The seasonal variation of the tropical circulation as simulated by a global model of the atmosphere, *J. Atmos. Sci.*, **31**, 43-83, 1974.

Manabe, S. and J. L. Holloway, Jr., The seasonal variation of the hydrologic cycle as simulated by a global model of the atmosphere, *J. Geophys. Res.*, **80**, 1617-1649, 1975.

Marenco, A., M. Macaigne, and S. Prieur, Meridional and vertical CO and CH_4 distributions in the background troposphere (70° N - 60° S; 0-12 km altitude) from scientific aircraft measurements during the STRATOZ III experiment (June 1984), *Atmos. Environ.*, **23**, 185-200, 1989.

Marenco, A. and F. Said, Meridional and vertical ozone distribution in the background troposphere (70° N - 60° S; 0-12 km altitude) from scientific aircraft measurements during the STRATOZ III experiment (June 1984), *Atmos. Environ.*, **23**, 201-214, 1989.

Moody, J. L., S. J. Oltmans, H. Levy II, and J. T. Merrill, Transport climatology of tropospheric ozone: Bermuda, 1988-1991, *J. Geophys. Res.*, **100**, 7179-7194, 1995.

Müller, J.-F. and G. Brasseur, IMAGES: A three-dimensional chemical transport model of the global troposphere, *J. Geophys. Res.*, **100**, 16,445-16,490, 1995.

Novelli, P. C., L. P. Steele, and P. P. Tans, Mixing ratios of carbon monoxide in the troposphere, *J. Geophys. Res.*, **97**, 20,731-20,750, 1992.

Novelli, P. C., K. A. Masarie, P. P. Tans, and P. M. Lang, Recent changes in atmospheric carbon monoxide, *Science*, **263**, 1587-1590, 1994.

Parrish, D. D, J. S. Holloway, M. Trainer, P. C. Murphy, G. L. Forbes, and F. C. Fehsenfeld, Export of North American ozone pollution to the North Atlantic Ocean, *Science*, **259**, 1436-1439, 1993.

Penkett, S. A., N. J. Blake, P. Lightman, A. R. W. Marsh, and P. Anwyl, The seasonal variation of nonmethane hydrocarbons in the free troposphere over the North Atlantic Ocean: possible evidence for extensive reaction of hydrocarbons with the nitrate radical, *J. Geophys. Res.*, **98**, 2865-2885, 1993.

Prinn, R., D. Cunnold, P. Simmonds, F. Alyea, R. Boldi, A. Crawford, P. Fraser, D. Gutzler, D. Hartley, R. Rosen, and R. Rasmussen, Global average concentration and trend for hydroxyl radicals deduced from ALE/GAGE trichloroethane (methyl chloroform), *J. Geophys. Res.*, **97**, 2445-2462, 1992.

Prinz, B., Ozone effects on vegetation, in Tropospheric Ozone: Regional and Global Scale Interactions, edited by Ivar S. Isaksen, D. Reidel, Dordrecht, Holland, 1988.

Rodhe, H. A. and I. S. A. Isaksen, Global distribution of sulphur compounds in the troposphere estimated in a height/latitude transport model, *J. Geophys. Res.*, **85**, 7401-7409, 1980.

Rudolph, J., B. Vierkorn-Rudolph, and F. X. Meixner, Large-scale distribution of peroxyacetylnitrate results from STRATOZ III flights, *J. Geophys. Res.*, **92**, 6653-6661, 1987.

Rudolph, J., Two-dimensional distribution of light hydrocarbons: results from the STRATOZ III experiment, *J. Geophys. Res.*, **93**, 8367-8377, 1988.

Rudolph, J., The tropospheric distribution and budget of ethane, *J. Geophys. Res.*, **100**, 11,369-11,381, 1995.

Schlesinger, W. H., Biogeochemistry: An Analysis of Global Change, Academic Press, San Diego, CA, 1990.

Schmitt, R. Simultaneous measurements of carbon monoxide, ozone, PAN, NMHC and aerosols in the free troposphere at Izaña, Canary Islands, In: *Proc. EUROTRAC Symposium '94*, ed. P. M. Borrell, P. Borrell, T. Cvitas, and W. Seiler, Garmisch-Partenkirchen, F. R. G., 11-15 April, 1994.

Schmitt, R. and P. Carretero, Ozone in the free troposphere over the North Atlantic: production and long range transport, to be published in *EUROTRAC Proceedings 1995*, 1995.

Seinfeld, J. H., Atmospheric Chemistry and Physics of Air Pollution, John Wiley & Sons, New York, 1986.

Simpson, D., Long-period modelling of photochemical oxidants in Europe. model calculations for July 1985, *Atmos. Environ.*, **26A**, 1609-1634, 1992.

Simpson, D., Photochemical model calculations over Europe for two extended summer periods: 1985 and 1989. model results and comparison with observations, *Atmos. Environ.*, **27A**, 921-943, 1993.

Simpson, D., Biogenic emissions in Europe 2. Implications for ozone control strategies, *J. Geophys. Res.*, **100**, 22,891-22,906, 1995.

Simpson, D., A. Guenther, C. N. Hewitt, and R. Steinbrecher, Biogenic emissions in Europe 1. Estimates and uncertainties, *J. Geophys. Res.*, **100**, 22,875-22,890, 1995.

Singh H. B., J. R. Martinez, D. G. Hendry, R. J. Jaffe, and W. B. Johnson, Assessment of the oxidant forming potential of light saturated hydrocarbons in the atmosphere, *Environ. Sci. Technol.*, **15**, 113-119, 1981.

Singh, H. B., L. J. Salas, B. A. Ridley, J. D. Shetter, N. M. Donahue, F. C., Fehsenfeld, D. W. Fahey, D. D. Parish, E. J. Williams, S. C. Liu, G. Hubler, and P. C. Murphy, Relationship between peroxyacetyl nitrate and nitrogen oxides in the clean troposphere, *Nature*, **318**, 347-349, 1985.

Singh, B., W. Viezee, and L. J. Salas, Measurements of selected C2-C5 hydrocarbons in the troposphere: latitudinal, vertical, and temporal variations, *J. Geophys. Res.*, **93**, 15,861-15,878, 1988.

Singh, H. B., D. O'Hara, D. Herlth, J. D. Bradshaw, S. T. Sandholm, G. L. Gregory, W. Schse, D. R. Blake, P. J. Crutzen, and M. A. Kanakidou, Atmospheric measurements of peroxyacetyl nitrate and other organic nitrates at high latitudes: possible sources and sinks, *J. Geophys. Res.*, **97**, 16,511-16,522, 1992.

Sladkovic, R. H. E. Scheel, and W. Seiler, Ozone climatology at mountain sites, Wank and Zugspitze, In: *Proc. EUROTRAC Symposium '94*, ed. P. M. Borrell, P. Borrell, T. Cvitas, and W. Seiler, Garmisch-Partenkirchen, F. R. G., 11-15 April, 1994.

Staehelin, J. and W. Schmid, Trend analysis of tropospheric ozone concentrations utilizing the 20-year ozone data set over Payerne (Switzerland), *Atmos. Environ.*, **25A**, 1739-1749, 1991.

Stockwell, W. R., P. Middleton, J. S. Chang, and X. Tang, The second generation regional acid deposition model chemical mechanism for regional air quality modeling, *J. Geophys. Res.*, **95**, 16,343-16,367, 1990.

Strand, A. and O. Hov, A two-dimensional zonally averaged transport model including convective motions and a new strategy for the numerical solution, , *J. Geophys. Res.*, **98**, 9023-9037, 1993.

Strand, A. and O. Hov, A two-dimensional global study of tropospheric ozone production, *J. Geophys. Res.*, **99**, 22,877-22,895, 1994.

Thompson, A. M., The oxidizing capacity of the Earth's atmosphere: probable past and future changes, *Science*, **256**, 1157-1165, 1992.

Tille, K. J. W., M. Savelsberg, and K. Bachmann, Airborne measurements of nonmethane hydrocarbons over western Europe: vertical distributions, seasonal cycles of mixing ratios and source strengths, *Atmos. Environ.*, **19**, 1751-1760, 1985.

Vaughan, G., Stratosphere-troposphere exchange of ozone. in Tropospheric Ozone: Regional and Global Scale Interactions, edited by Ivar S. Isaksen, D. Reidel, Dordrecht, Holland, 1988.

Venkatram, A., P. K. Karamchandani, and P. K. Misra, Testing a comprehensive acid deposition model, *Atmos. Environ.*, **22**, 737-747, 1988.

Vögtlin, R. M. Löffler-Mang, m. Koßman, U. Corsmeier, F. Feidler, O. Klemm, and H. Schlager, In: *Proc. EUROTRAC Symposium '94*, ed. P. M. Borrell, P. Borrell, T. Cvitas, and W. Seiler, Garmisch-Partenkirchen, F. R. G., 11-15 April, 1994.

World Meteorological Organization (WMO), Scientific assessment of ozone depletion: 1991, Rep. 25, WMO Global Ozone Research and Monitoring Project, Geneva, 1992.

Zander, R., P., Demoulin, D. H. Ehhalt, U. Schmidt, and C. P. Rinsland, Secular increase in the total vertical column abundance of carbon monoxide above central Europe since 1950, *J. Geophys. Res.*, **94**, 11,021-11,028, 1989.

Zimmerman, P. H., MOGUNTIA: a handy global tracer model, In: *Proc. 16th NATO/CCMS Int. Tech. Mtg. Air Pollution Modeling and its Application*, Lindau F. R. G. 6-10 April 1987.

Zimmerman, P. H., J. Feichter, H. K. Rath, P. J. Crutzen, and W. Weiss, A global three-dimensional source-receptor model investigation using ^{85}Kr, *Atmos. Environ.*, **23**, 25-35, 1989.